ANALYSIS AND OPTIMIZATION USING NUMERICAL AND EXPERIMENTAL EVALUATION METHODS FOR MULTIDISCIPLINARY DESIGN PROBLEMS

A Record of Study

by

BONG TAEK OH

Submitted to the Office of Graduate Studies of
Texas A&M University
in partial fulfillment of the requirements for the degree of

DOCTOR OF ENGINEERING

May 2009

Major Subject: Engineering
College of Engineering

ANALYSIS AND OPTIMIZATION USING NUMERICAL AND EXPERIMENTAL EVALUATION METHODS FOR MULTIDISCIPLINARY DESIGN PROBLEMS

A Record of Study

by

BONG TAEK OH

Submitted to the Office of Graduate Studies of
Texas A&M University
in partial fulfillment of the requirements for the degree of

DOCTOR OF ENGINEERING

Approved by:

Chair of Committee,	Dimitris C. Lagoudas
Committee Members,	John Whitcomb
	Ramesh Talreja
	Terry Creasy
Coordinator, College of Engineering,	Robin Autenrieth

May 2009

Major Subject: Engineering
College of Engineering

ABSTRACT

Analysis and Optimization Using Numerical and Experimental Evaluation Methods for Multidisciplinary Design Problems. (May 2009)

Bong Taek Oh, B.S., SoongSil University;

M.S., SoongSil University

Chair of Advisory Committee: Dr. Dimitris C. Lagoudas

The Multidisciplinary Design Optimization (MDO) system is needed to reduce the developing time and production cost in most industries. The MDO is the new technology for optimization design, and considers solid mechanics, dynamics, kinematics, vibration/noise control, and fluid mechanics, simultaneously. Higher product quality, less developing time and lower manufacturing cost will be achieved through a balanced and organic MDO method. In this paper, numerical stress analysis, optimization method, and experimental stress analysis will be conducted to accomplish: 1) production cost; 2) developing time; 3) quality improvement; and 4) service-rate drop. First, the coupled analysis using the finite element method will be performed to obtain the accurate data. Second, OPTISTRUCT®, which is commercial optimization software, will be used for shape and size optimization analysis. Third, an experimental stress analysis system will be established to assist the optimization design and numerical analysis.

TABLE OF CONTENTS

CHAPTER Page

LIST OF FIGURES

FIGURE Page

LIST OF TABLES

CHAPTER I

INTRODUCTION

The design process – and especially the process of designing complicated products – is managed by many design and analysis teams. When an air purifier is designed, for example, designers will be needed to design the fan, including the blade and case, front and back covers, fan insert, and electrical devices. The analysis team usually consists of specialists with expertise on structural strength, fluid flow, noise/vibration control, and dynamic analysis. Sometimes drop analysis may be included as well, if it is part of the design specification. Fig. 1 shows the typical product development procedure, from the product planning step to the final design review step. If the analysis starts after the first draft of the design is finished (D+35 in DR-1 process as shown in Fig. 1), the analysis team will have only seven working days to submit the first report (D+41 in DR-1 process as shown in Fig. 1). Therefore, it is very important to work with the analysis simultaneously in order to complete the job well and on time. The design team should give all needed information about the design concept and limit to the analysis team. Also, the analysis team should let the design team know not only of the factors which can affect the products considerably, but also of the influence of the analysis results. The design team will then effectively utilize this information in their product design.

The development process is shown as a one-way procedure in Fig. 1. However, this is not the case in the real world, because the factors we should consider are too complicated to complete the design in one cycle. The re-design process is meant to fix the design flaws and improve the product performance. The re-design process usually takes a long time, as it involves

---

This record of study follows the style of *AIAA Journal*.

feedback from all design and analysis teams in order to optimize and confirm each team's opinion. Therefore, the Multidisciplinary Design Optimization (MDO) system [1, 2] is needed to reduce the total product developing time and production cost [3-7].

The MDO is the new technology for optimization design, and considers solid mechanics, dynamics, kinematics, vibration/noise control, and fluid mechanics simultaneously. Higher product quality, shorter developing time, and lower manufacturing costs will be achieved through a balanced MDO method. Fig. 2 shows the flow chart and the framework of MDO technology. Three optimization systems will be constructed to accomplish the following: 1) lowering of production cost; 2) decrease of developing time; 3) improvement of quality; and 4) service-rate drop.

First, the numerical analysis for manufacturing of products will be performed. The injection-molding method is usually used to make plastic products. High temperatures are needed to melt plastics (e.g. ABS, Noryl, and PP), and these high temperatures generate considerable residual stress. The residual stress data obtained from the injection-molding analysis will be used for structural strength analysis. The structural-fluid coupled analysis will be also used for the optimization system.

Second, OPTISTRUCT®, which is a commercial optimization software, will be used for topology and topography optimization, as well as shape and size optimization analysis. OPTISTRUCT® is a finite element-based structural analysis and optimization software tool that is used to design and optimize structures by formulating the objectives and constraints with one or more of the following responses: 1) compliance; 2) frequency; 3) volume; 4) mass; 5) displacements; 6) buckling factor; 7) stresses, strains, forces, and complex failures; and 8) user-defined responses and properties. The basic analysis features include linear static analysis, normal modes analysis, linear buckling analysis, and frequency response analysis, which use the

direct modal method.

Third, an experimental stress analysis system will be established in order to confirm and correlate with the structural stress analysis and optimization results. The experimental analysis systems including universal test system (UTS), internal pressure test system, thermal deformation test system, noise analysis system, and drop test system will be used. The correlation between numerical and experimental results will be utilized to maximize product quality and optimize the size, shape, and material type.

See Figures 1 and 2 below.

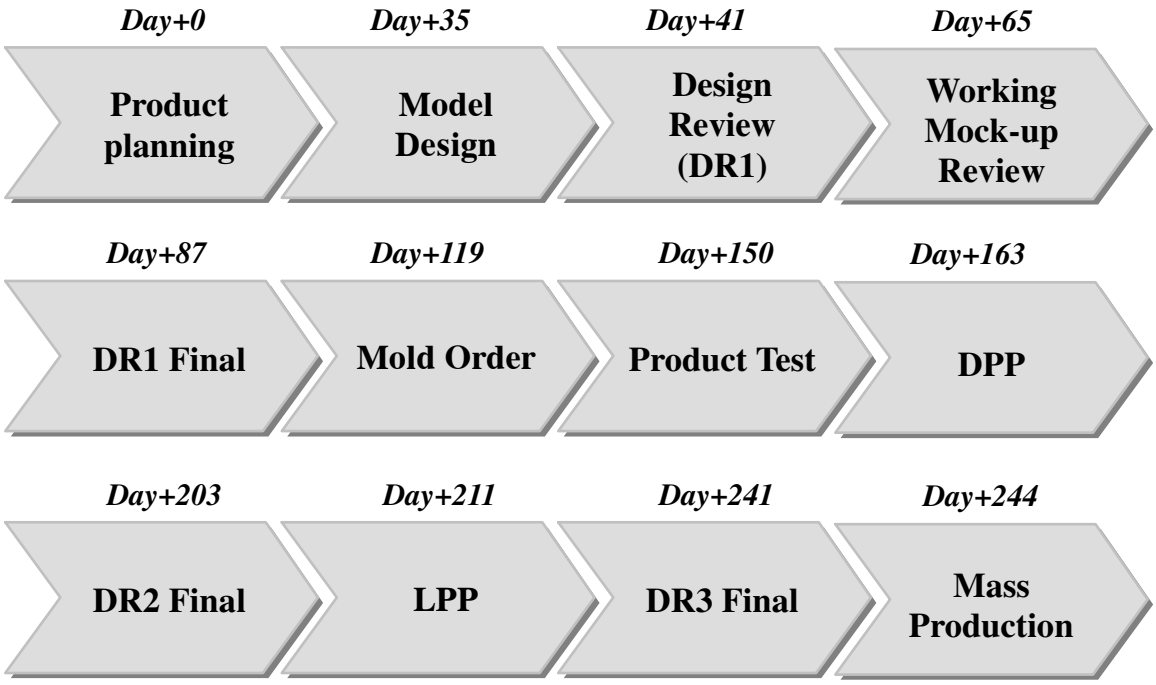

Fig. 1 Typical product development process

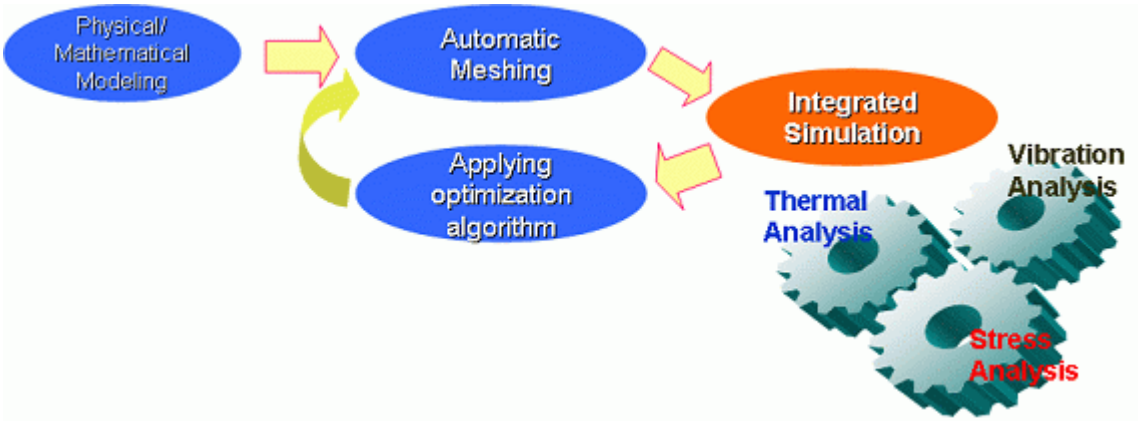

(a) Flow chart

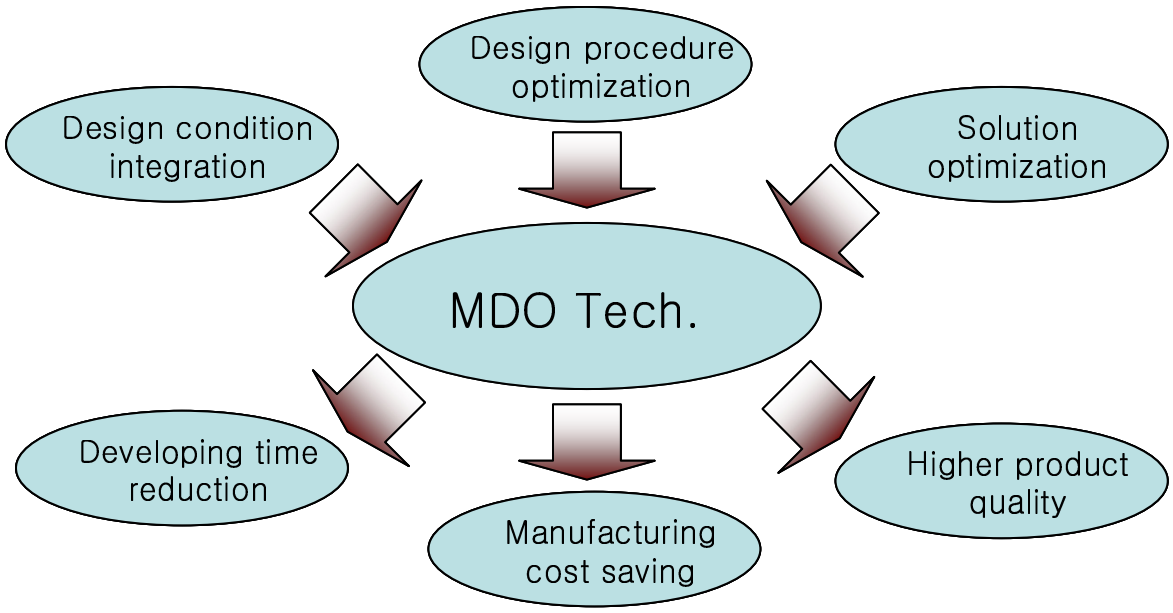

(b) Framework

Fig. 2 Schematic explanations of MDO technology

The core technical research & development division operates two separate research teams, which are the CAE (computer-aided engineering) team and the experimental evaluation team. I have a responsibility for both of teams, and the responsibility involves an engineering design analysis and middle-level management. Five different projects are performed in this report as follows: 1) New insert design for air-purifier; 2) Cost reduction using injection molding analysis; 3) Structural analysis for ion exchange tank; 4) Cost reduction using shape optimization; 5) CAE involved development process. I execute numerical and experimental stress analysis, and also manage both the CAE [8, 9] and the experimental evaluation team members during all projects. In this report, the analysis and optimization methods that use numerical and experimental evaluation techniques for multidisciplinary design optimization (MDO) will be summarized for five projects. The software used for the projects are ALGOR and ANSYS for structural analysis, 3-D TIMON for injection molding analysis, and OPTISTRUCT for shape optimization. The CATIA is used as a CAD (Computer Aided Design) tool.

CHAPTER II

INTERNSHIP POSITION

Living supplies manufacturers are endlessly looking for ways to make their products safer, lighter weight and more cost effective. As restraint and safety systems get more sophisticated, the new advanced systems are expected to be incorporated without affecting the overall cost of a product, Therefore, constant improvement in the efficiency of restraint system is necessary.

Woongin coway is a leading well-being household electronic appliances manufacture in Korea. Coway has promoted a healthy and comfortable life for consumers as its meaning suggest; always together. Coway products include air purifiers, water filtration devices, digital bidets, megasonic cleaning device, and other well-being home appliances. Coway's industry-leading market share in Korea ranges from over 50 percent for water filtration devices to 40 percent for air purifiers. Currently, more than one out of four Koreans use Coway water filtration devices, and one out of ten uses Coway's air purifiers. Last year, Coway achieved KRW 1.117 billion(USD 1.2 billion) in revenue, representing a 10.9 percent increase from the year before.

Research and development innovation at Woongjin Coway is focused primarily on delivering improved consumer convenience rather than improved profit for the company. In other words, R&D is founded on consumer-centric system that exhaustively identifies and discovers consumer needs in product development. As of the end of 2007, total 250 R&D personnel(18 doctorate and 84 master degrees) concentrate on R&D institute of Woongjin Coway. Last year Woongjin Coway applied for total 195 patents and registered 44 patents as shown in Fig. 3.

In February 2008, Woongjin Coway completed construction of the 'Woongjin Coway R&D Center.' Installed with high-tech facilities, Coway has secured the largest home appliance research center in Korea. Through the completion of the R&D Center for which an amount of

KRW 58 billion was invested, the largest amount among all research facilities in the Seoul National University, Coway is now capable of obtaining excellent personnel in advance. By combining our R&D space and personnel which was dispersed in Seoul, Incheon, and Gongju Cungnam, Coway is able to conduct more efficient and concentrated research. The R&D center, whose ownership will be transferred to Seoul National University 20 years from now, is assessed as a representative case in academic-industrial cooperation. Coway also agreed to provide an annual amount of KRW 500 million as scholarship for the next 15 years, which will reach an amount of KRW 7.5 billion.

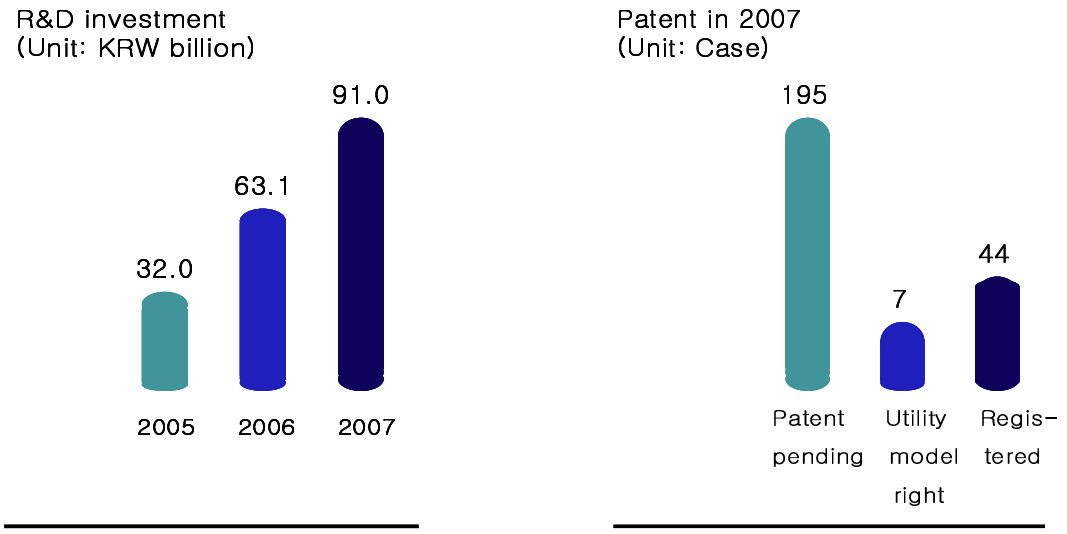

Fig. 3 R&D investment and patent status of Coway

From this internship, I learned about and gained practical experience in engineering design and analysis, and middle-level management procedures. I was hired as a project researcher in the Woongjin Coway Co. for the entire 2006 calendar year. My job duties entailed solving technical problems in engineering design, and I assisted the senior project researcher in training, disciplining, and motivating research team members.

My working experience was divided into two sections, engineering design analysis and middle-level management. The core technical research & development division operates two separate research teams, which are the CAE (computer aided engineering) team and the experimental evaluation team. I will work in both CAE and the experimental evaluation team.

CHAPTER III

PROJECT 1: NEW INSERT DESIGN USING THERMOMECHANICAL STRESS ANALYSIS

3.1 Finite Element Model

- Problem Description

Fig. 4 shows the air purifier (The model name is Venus) and the direction of the air flow. The motor is located at the center of the fan and it has about 70°C of temperature while running. The insert is attached to the fan of air purifier using injection molding method. The shaft of motor is placed in the insert. The thermal stress may occur as a result of the difference in the thermal expansion coefficient [10-14], because the fan is made of plastic (ABS) and the insert is made of brass. Experimental tests were carried out under extreme conditions – namely, air purifiers were turned on for 24 hours at the highest speed with a one-hour turnoff period to allow the machine to cool down – and a crack occurred between the insert and the fan after 375 hours as shown in Fig.4. The purpose of this project is to find the proper material and shape for both the fan and the insert in order to obtain the required structural strength.

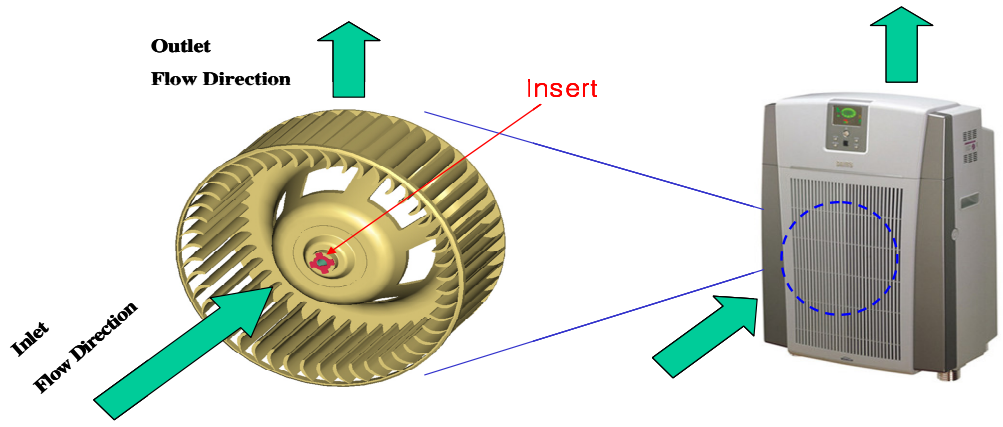

Fig. 4 Venus model of air purifier from Woongjin Coway Co.

The fan is designed to suck outside air into the air purifier and to send out the clean air after purification process has been completed, as shown in Fig. 4. The fan has a washer and inserts that connect to the motor, as shown in Fig. 5. The washer and insert are made of brass and are directly connected to the motor. The insert is implanted when the fan is made via an injection molding method. The washer is fastened with a nut. The motor shaft reaches temperatures of 70°C, due to the high temperature from the driving part inside of the motor. The thermocouples are used to obtain the temperature at several points near the insert, and the convection coefficient is analyzed using FEA (Finite Element Analysis) with the temperature obtained from the thermocouples. The net weight of the fan is 1450g, and the rate of rotation for the motor is 730 rpm. Three different loading conditions are used for the investigation using FEA: 1) Loading condition 1 (LC1), rotation loading condition with net weight under 70°C; 2) Loading condition 2 (LC2), thermal condition (70°C) only; 3) Loading condition 3 (LC3), rotation loading condition with net weight under room temperature.

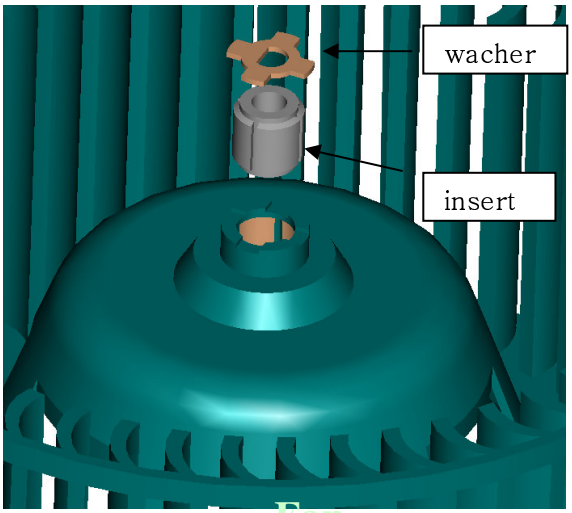

Fig. 5 Image showing fan, inserts, and washer

The commercial finite element analysis software ALGOR is used for thermomechanical analysis. ALGOR has a high compatibility with OPTISTRUCT program, which is optimization software. OPTISTRUCT will be explained in detail in Chapter Ⅵ. The convergence study is performed to determine the required number of elements, and the 1,000,000 of elements are obtained. The eight-node coupled thermal-stress elements are used to investigate both temperature distribution and stresses for all loading conditions. The inside of the insert can reach 70ºC from the shaft of motor, which is the source power of torque. The upper part of the washer (point A in Fig. 6) reaches 60ºC, which has been determined by experiments using thermocouples.

Many factors, such as the materials used, the shape of the inserts, the types of motors used, and the injection molding conditions, can affect the temperature profile and local stress level. In this project, two different materials were used and several different shapes of inserts were examined, as shown in Table 1. The air purifier (product model name is VENUS) is failed in field test and the problem is the crack initiation between the insert and the fan. The object of this project is to reduce the thermal stress to prevent the crack initiation between the insert and the fan, and the manufacturing cost should be also maintained. The current motor used in this product is the AC motor. The BLDC motor could be a candidate to reduce the applied temperature; however, the cost of BLDC motors is too high, and the design for new electric circuit will take a good deal of time. Therefore, considering BLDC motors were excluded.

Table 1 Shapes of inserts and used materials

Materials	Thermal Expansion Coefficient	Types of Inserts
Copper	1.8 X 10-6 mm/mm/°C	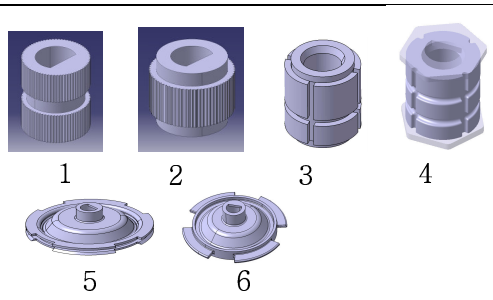
Aluminum	2.37 X 10-6 mm/mm/°C	

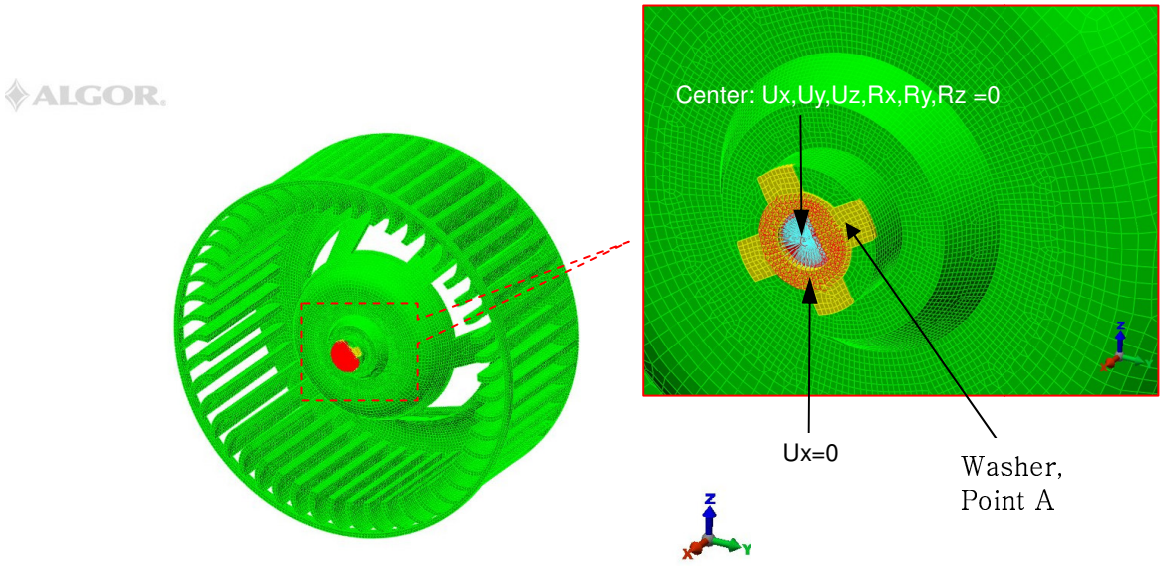

Fig. 6 Fan model and boundary conditions

The center of shaft is fixed using spider links, and the boundary conditions on the upper part of shaft can be expressed as shown in Fig. 6. The contact boundary conditions are applied as shown in Fig. 7.

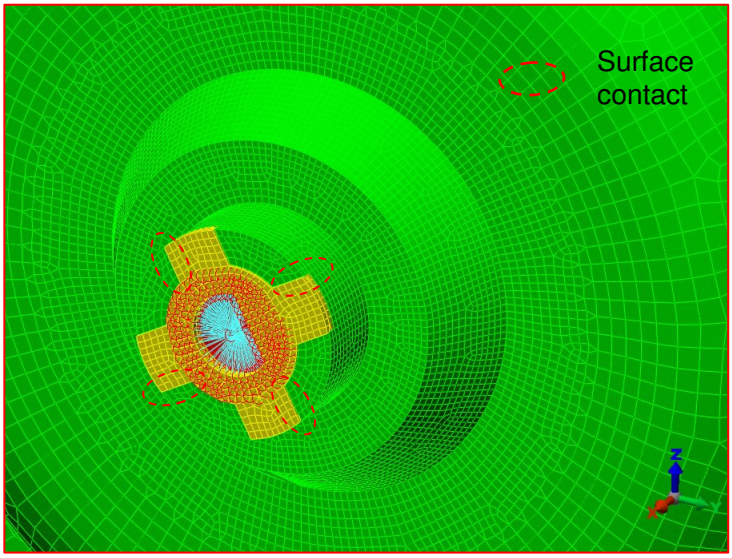

Fig. 7 Contact boundary conditions between washer and fan

- Finite Element Analysis Procedure

To investigate the effects of the shapes and material properties in the context of the study of thermal stress between the fan and the insert, the thermomechanical analysis will be explained in the next section using FEA. In this section, the flow chart for FEA is shown, as illustrated in Fig. 8. CATIA (computer aided three dimensional interactive application) is one of 3-D CAD tools, and it is wildly used in aerospace and automobile industries. HYPERMESH is a high-performance finite element pre-processor that provides a highly interactive & visual environment to analyze product design performance. First, the geometry must be edited, using CATIA and HYPERMESH to remove unnecessary fillets, parts, and bosses etc. The model also must be simplified in order to save meshing time before the FEA model can be made. Next, the finite element model will be created and the boundary/loading conditions and material properties will be applied, using HYPERMESH. The file is transferred to the ALGOR solver after the mesh

quality is checked for better results. Many factors (material properties, insert shapes, motor types etc.) that affect the thermal stresses near the insert edges must be carefully examined in order to understand the effect of the thermal expansion coefficients between two materials.

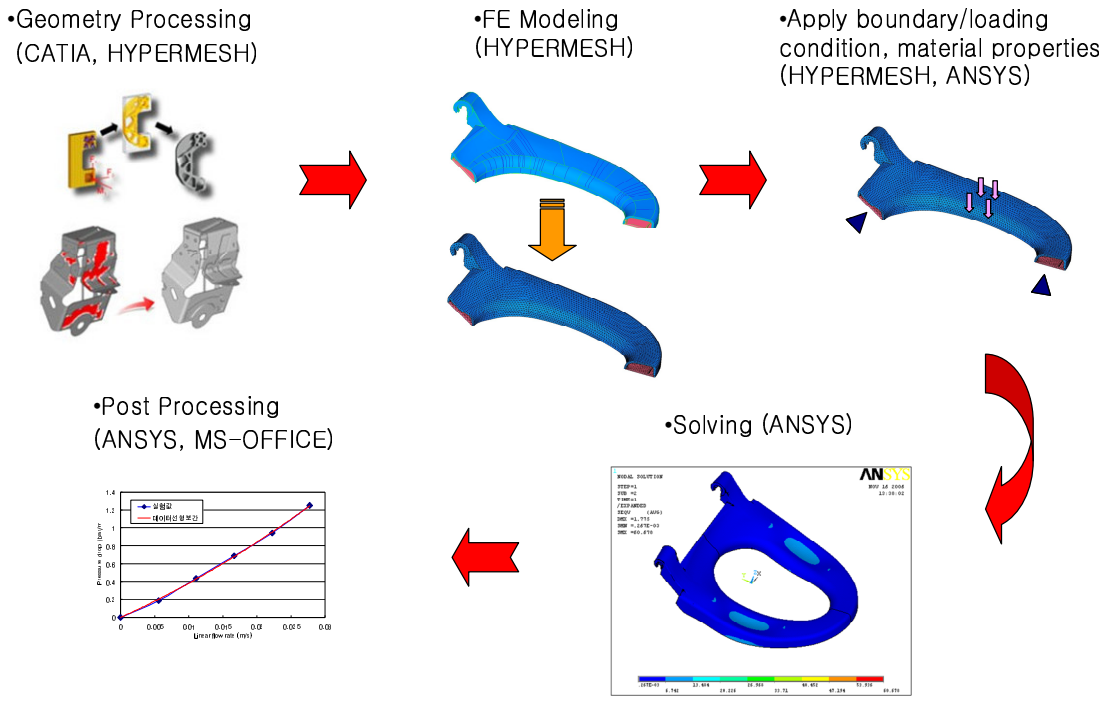

Fig. 8 Flow chart of the finite element analysis for each step

3.2 Temperature Distribution

The insert is placed in the fan using injection molding method as explained in section 3.1. The thermal loading is occurred during the injection molding as a boundary condition, therefore the injection molding method must be explained to understand a boundary condition.

The injection molding method is used to shape plastic resins for making the fan of air purifier systems. The resin is heated up to 230°C to melt the plastic (ABS), and cooled down to room temperature. This temperature difference may cause a residual stress. Residual stress is a

process-induced stress [15], which exists in a molded part. It can be either flow-induced or thermal-induced. Residual stresses have an effect on a part similar to externally applied stresses. If the residual stresses are strong enough to overcome the structural integrity of the part, the part will twist upon ejection, or later crack, when external service load is applied. Residual stresses are the main cause of part shrinkage and warpage. The process conditions and design elements that reduce shear stress during cavity filling will help to reduce flow-induced residual stress. Likewise, those that promote sufficient packing and uniform mold cooling will reduce thermal-induced residual stress. For fiber-filled materials, those process conditions that promote uniform mechanical properties will reduce thermal-induced residual stress. To reduce the flow-induced residual stress [16, 17], the following methods are used.

1) higher melt temperature;
2) higher mold-wall temperature;
3) longer fill time (lower melt velocity);
4) decreased packing pressure;
5) shorter flow path;

Conditions that lead to sufficient packing and more uniform mold-wall temperatures will reduce the thermal-induced residual stresses. These include:

1) Proper packing pressure and duration
2) Uniform cooling of all surfaces of the part
3) Uniform wall-section thickness

The above injection molding techniques are used to minimize residual stress. Therefore, it is assumed that residual stress is nearly zero, or that all models in this paper have similar levels of residual stress. To investigate the effects of the high temperature from the motor, a thermomechanical analysis was performed using FEA in this section. The temperature contour

plot of the computational domain is shown in Fig. 9, in which a large temperature gradient can be seen near the edge of the insert.

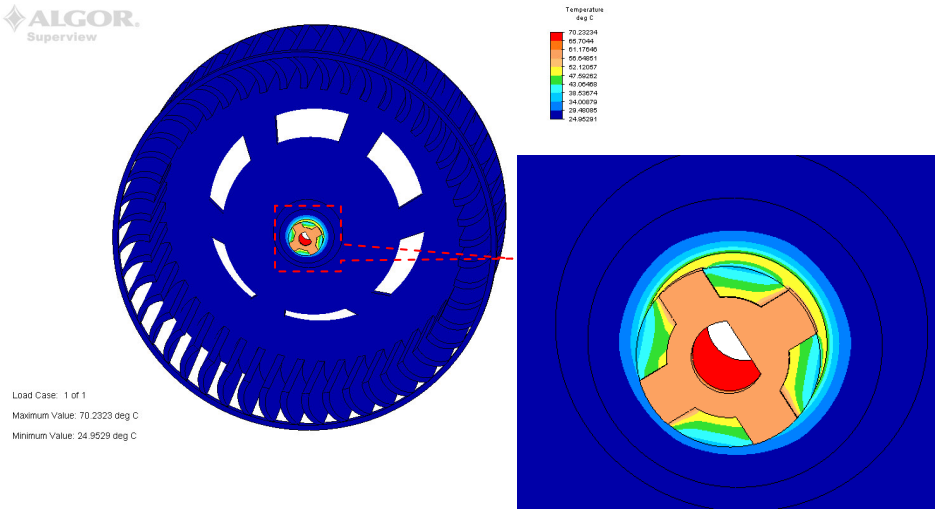

Fig. 9 Temperature distribution of the fan

3.3 Thermomechanical Stress Analysis

The von Mises criterion is often used to estimate the yield of ductile material, and it is also known as the maximum distortion energy criterion [18], octahedral shear stress theory, or Maxwell-Huber-Hemoky-von Mises theory.

The von Mises criterion states that failure occurs when the energy of distortion reaches the same energy for yield/failure in uniaxial tension. In other words, the von Mises yield criterion says that yielding occurs when the von Mises stress exceeds the yield strength in tension. The von Mises stress is widely used in Finite Element Analysis (FEA) as the metric for assessing design margins for ductile materials Such as metals [19, 20]. Although the von Mises yield criterion originated for metals, it has been used successfully to predict load-deflection behavior in thermoplastic parts experiencing yielding [21]. The difference between yielding in thermoplastic and metals is the state of stress upon yielding. Unless subject to high pressure, the

yield stress of metals depends only on the deviatory stress tensor and therefore follows the von Mises criterion.

The yield stress of thermoplastic depends also on the hydrostatic components of the stress tensor. A modified criterion has been recommended for plastic materials [22-24]. Therefore, von Mises stress is used to predict the initiation of failure where the highest stress occurred. In this report, the crack growth (after the initiation of crack) will not be studied. The von Mises stress instead of fracture toughness, which is usually used for the evaluation of crack growth, will be used to detect the weakest point of the structures.

Fig. 10 shows the von Mises stress profile on the fan for loading case 1space (LC1), where it can be seen that there is a large concentration of stress on the interface between the washer and the fan. It is also shown that there is high stress on the interface between the fan and the insert.

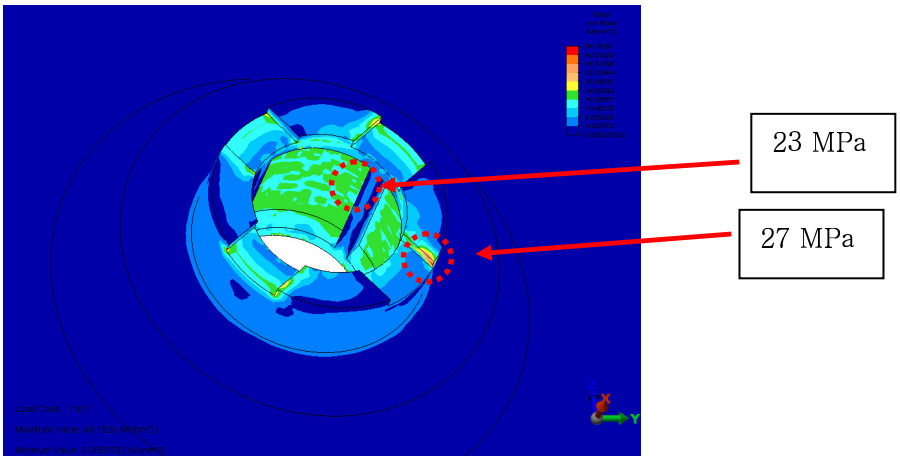

Fig. 10 Stress distributions near the insert on the fan

The comparison of LC1, LC2, and LC3 is shown in Table 2. According to the result, as shown in Table 2, the effects of weight and torque are negligible as compared with that of the temperature from the motor shaft. The tensile strength of ABS is 50.24 MPa, and the poison's ratio is 0.35. When we consider the safety factor of the plastics, its effective strength will be 25.26 MPa. Therefore, the stress concentration for LC1 and LC2 on the fan is higher than the fan's effective strength. Different insert designs, materials, and boundary conditions (e.g. different motor types) should be considered in order to reduce the von Mises stress. Therefore, two different materials made of copper and aluminum were used to investigate the effect of the thermal expansion coefficient between the insert and fan. Several different insert types were also considered to reduce the von Mises stress, as shown in Table 1. Fig. 11 shows the von Mises stress between the insert and fan for the insert type 6 in Table 1, and it shows that the highest stress is decreased by 10% in model 6 as compared with model 1, as demonstrated in Fig. 10.

Table 2 Results for different loading conditions

	LC1	LC2	LC3
Von Mises Stress	27.1 Mpa	26.3 MPa	0.8 MPa

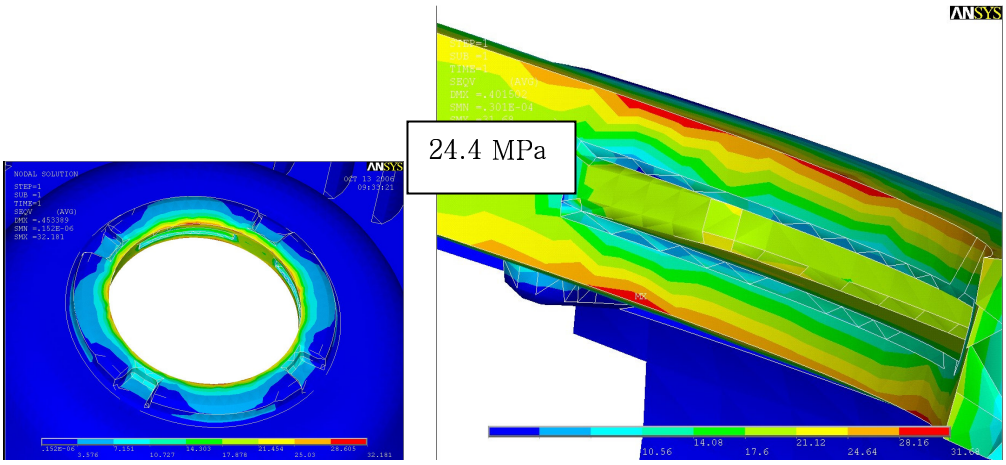

Fig. 11 Von Mises stress near the insert edge for model 6

To reduce the local stress and make injection molding easier, five more models for insert type 6 were considered as shown in Table 3. Three different angles of wing insertions were used and the corner of the wing was rounded, as shown in Fig. 12. Table 3 shows the result from thermomechanical stress analysis using ANSYS, and the von Mises stress of model 4 in Table 3 is decreased by 3.4 MPa.

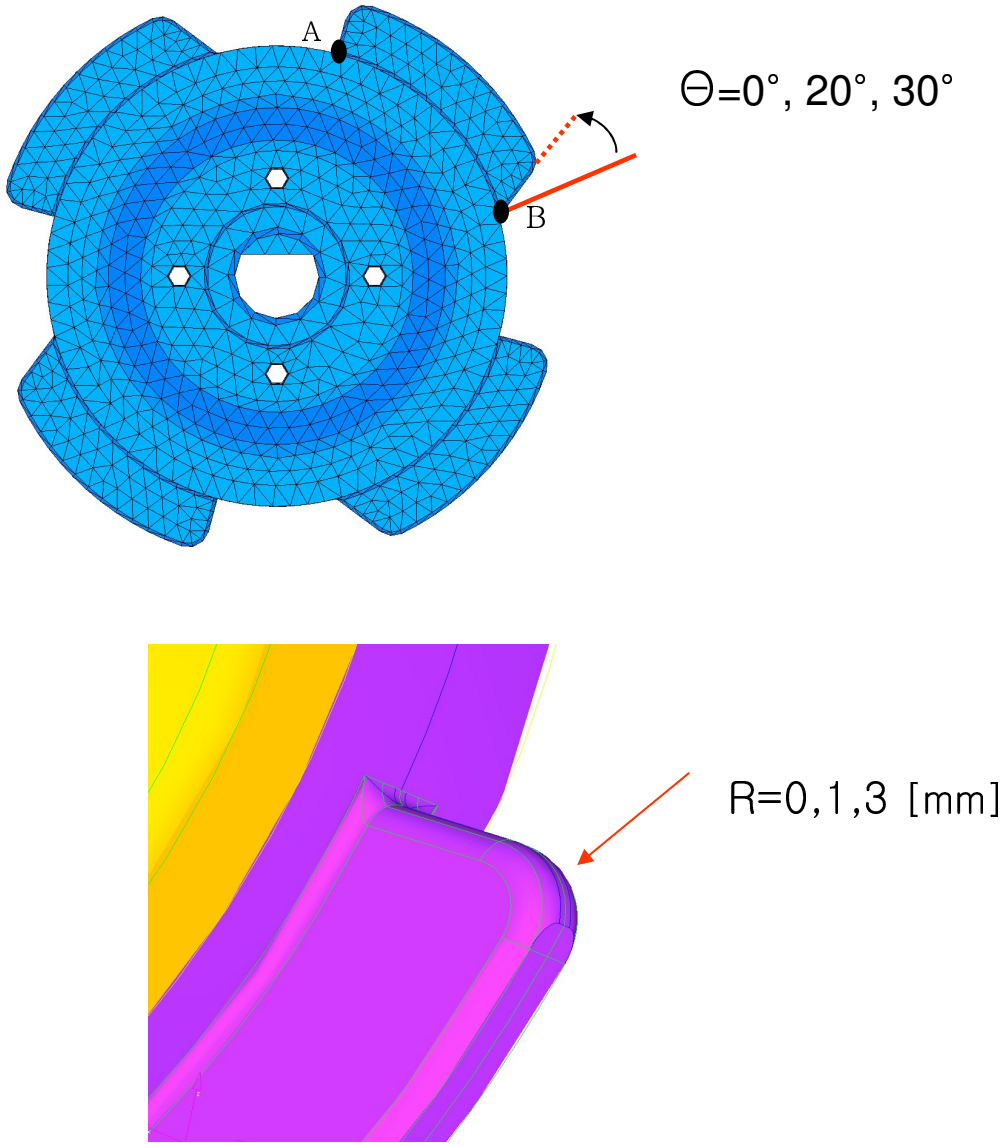

Fig. 12 Specimen configurations for aluminum insert

Table 3 Maximum von Mises Stress near the insert edge for aluminum insert models

	Model	Temp(℃)	von-Mises stress at contact area (MPa)		Injection molding analysis
			A	B	
0	Venus(copper insert)	70	30		
1	model 1(θ=30°, R=0mm)		25	23	
2	model 2(θ=0°, R=1mm)		24.4	24.4	Yes
3	model 3(θ=0°, R=3mm)		23.7	23.7	
4	model 4(θ=20°, R=3mm)		24	21	Yes
5	model 5(θ=30°, R=3mm)		23.5	22	Yes

3.4 Verification Using Reliability Test and Cost Savings

This section discusses how the different running speeds and weight balances of respective fans affect their product lives. The reliability test, using actual fans and inserts, will also verify the results of the numerical analysis. Table 4 shows the materials, inserts, and test conditions that are used in the actual reliability test. The air purifier is used for 2.25 hours a day under normal usage circumstances based on the consumer report, and it has one year warranty. Therefore, the test is stopped after 820 hours which is one year usage of the air purifier. The test results show that only one test specimen had a crack near the edge of the insert after 512 hours running with the aluminum insert type, and no crack was found after 820 hours in 15 other specimens. With the copper insert type, about half of the specimens had a crack after 820 hours. Separate from these eight, three specimens had a crack after either 374 or 650 hours. The difference in the thermal expansion coefficient may contribute to this result, since aluminum has a higher thermal expansion coefficient than copper has. The difference in the thermal expansion coefficient between the ABS and the aluminum is lower than the thermal stress between the fan and insert

when the motor is running with 70° of temperature is lower.

Table 4 Results of reliability test according to material properties and insert types

Material	Insert Type	Specimen Number	850rpm, W/B; 3.0g		950rpm, W/B; 3.0g		850rpm, W/B; 4.5g		950rpm, W/B; 4.5g	
			failure	time	failure	time	failure	time	failure	time
Aluminum	Type 1	#1 - #4	No	N/A	Yes	512	No	N/A	No	N/A
		#5 - #8	No	N/A	No	N/A	No	N/A	No	N/A
		#9 - #12	No	N/A	No	N/A	No	N/A	No	N/A
		#13 - #16	No	N/A	No	N/A	No	N/A	No	N/A
Copper	Type 2	#1 - #4	crack	820	No	N/A	No	N/A	crack	820
		#5 - #8	crack	820	crack	374	No	N/A	No	N/A
		#9 - #12	crack	650	crack	650	crack	820	crack	820

Type 1: 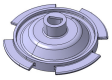 Type 2:  W/B: weight balance

The thermal loading from the motor shaft is a dominant factor under various loading conditions as explained in section 3.1. The crack is generated after 374 hours with a copper insert. With Aluminum material using new shape of insert, no crack occurred after 820 hours. The importing and editing method from CATIA (CAD software) to ALGOR (structural analysis software) is established for 3-D sold model. The complicated 3-D solid model can be easily and quickly meshed using Hyper mesh.

CHAPTER IV

PROJECT 2: COST REDUCTION USING INJECTION－MOLDING ANALYSIS

4.1 Injection Molding Method

The plastics are widely used in most industries such as living supplies, automobiles, computers, cell phones, and even in aerospace field. Most basic difference in polymers is made between thermoplastics and thermosets. Thermosets cannot be re-melted due to their chemical structure. When reheating they undergo a chemical alteration and the material changes. Thermoplastics on the contrary can be re-melted, when doing so, their structural properties change [25-29]. Only thermoplastics will be considered here. One of the most common methods of shaping plastic resins is a process called injection molding [30-32]. The second project involves injection molding analysis [33-35]. Injection molding is accomplished by large machines that are called injection-molding machines as shown in Fig. 13.

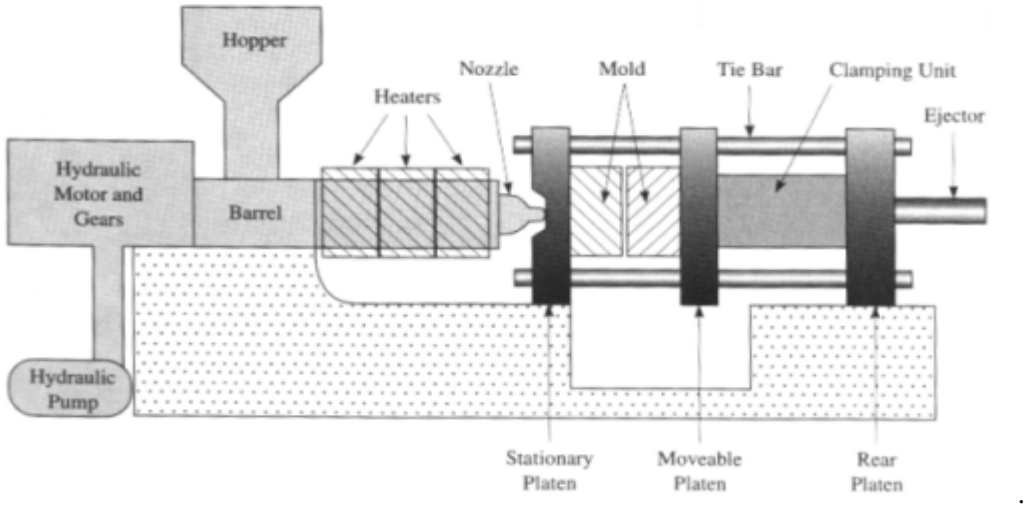

Fig. 13　Typical injection molding machine

Resin is fed to the machine through the hopper. Colorants are usually fed into the machine directly after the hopper. The resins are pulled by gravity through the feed throat into the

injection barrel. Upon entrance into the barrel, the resin is heated to the appropriate melting temperature. The resin is injected into the mold by a reciprocating screw or a ram injector. The reciprocating screw apparatus is shown above. The reciprocating screw offers the advantage of being able to inject a smaller percentage of the total shot (the amount of melted resin in the barrel). The ram injector must typically inject at least 20% of the total shot, while a screw injector can inject as little as 5% of the total shot. This means that the screw injector is better suited for producing smaller parts. The mold is the part of the machine that receives the plastic and shapes it appropriately. The mold is cooled constantly to a temperature that allows the resin to solidify and be cool to the touch. The mold plates are held together by hydraulic or mechanical force. The clamping force is defined as the injection pressure multiplied by the total cavity projected area. Typically molds are overdesigned depending on the resin to be used. Each resin has a calculated shrinkage value associated with it.

4.2 Description of Problem

Fig. 14 shows a typical water purifier from WoongJin Coway Co.; it has about 82,320 cm^2 of product size and 18 Kg of weight. The customer's need for a small product has been increasing rapidly in domestic markets, as well as overseas. In particular, customers in Europe and Japan demand small, light products. Also, the performance should be better and the customers prefer affordable price. The use of inexpensive materials is one of the ways to make the product low-price. At the same time, the product should have same or higher strength, product life, and molding ability. The injection molding analysis will be performed to keep the good molding ability and the use of low-price materials.

Fig. 14 Water purifier (cool and hot water)

When the water purifier is used, a place to put one's cup is needed. This place is called a tray grill. The tray grill is made of plastics, and the injection molding method is usually used to make it. Fig. 15 shows typical tray grill; it has many holes to drain water, and these holes may contribute to weld lines, which make the tray grill fragile and reduce the quality of its exterior. PC, or polycarbonate, is a material that is frequently used in tray grills. However, the use of ABS (Acylonitrile Butadiene Styrene) would reduce the cost, because PC is quite expensive material. In this chapter, an injection-molding analysis will be performed on the use of different materials that may reduce the production cost of tray grill.

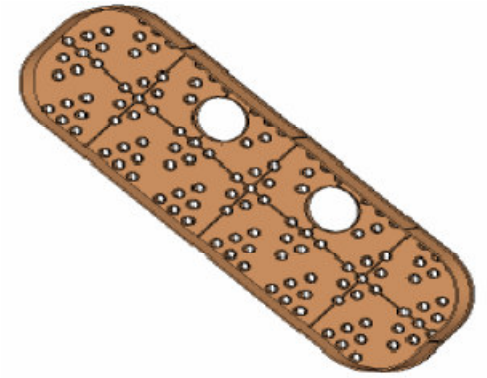

Fig. 15 Typical tray grill

4.3 Injection Molding Analysis

Fig. 16 shows the flow chart for the injection molding analysis, and HYPERMESH was used to build a tetra mesh. The 3D-TIMON, which is a commercial finite element analysis software, was used as a solver.

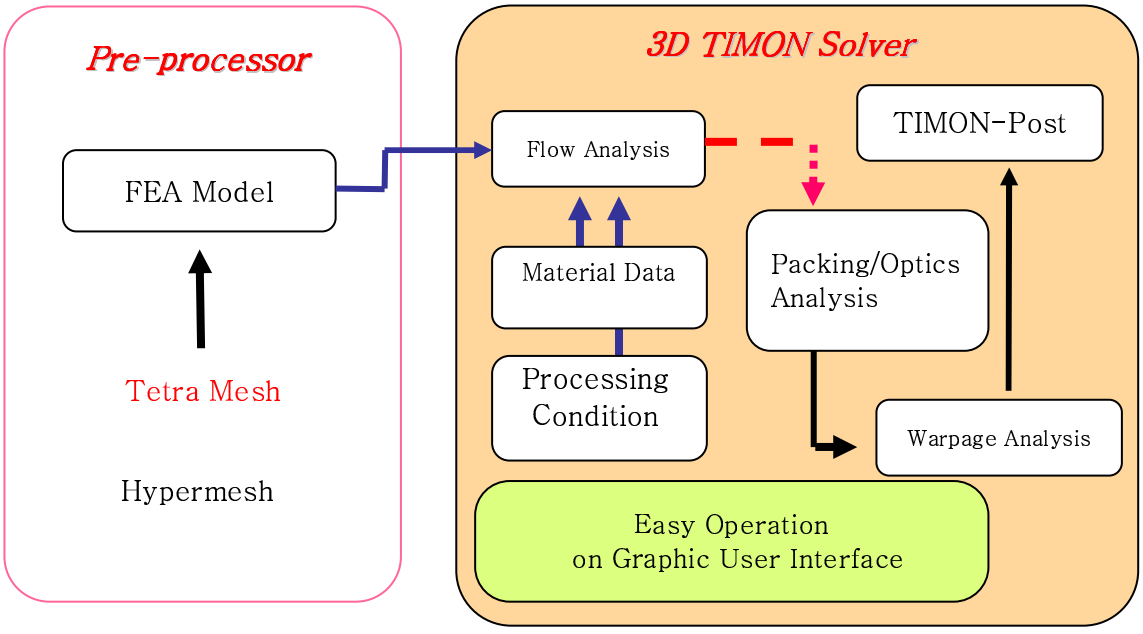

Fig. 16 Flow chart for injection molding analysis

To investigate the effect of the injection velocity, packing pressure, and delivery system, the injection molding analysis results will be explained in this section using FEA. First, the geometry must be edited, using CATIA and HYPERMESH, in order to remove unnecessary fillets, parts, and bosses. The model also needs to be simplified so as to save meshing time before the FEA model can be made. Next, the finite element model will be created and applied to the injection molding conditions, such as positions and number of gates. The file will be transferred to the 3D-TIMON solver after the mesh quality is checked for better results. The filling pattern, weld line, air trap, and deformed shape must be carefully examined to optimize the processing conditions.

4.4 Analysis Results under Various Molding Conditions

- Delivery System & Filling Pattern

Fig. 17 shows the analysis model and delivery system, and it has three tunnel gates on the side of the products. Each gate is 2mm in diameter, and the specifications of delivery system are shown in Fig. 17. The sprue has a diameter of 3.5mm of at the start point and a diameter of 9mm at the contact point between the sprue and runner.

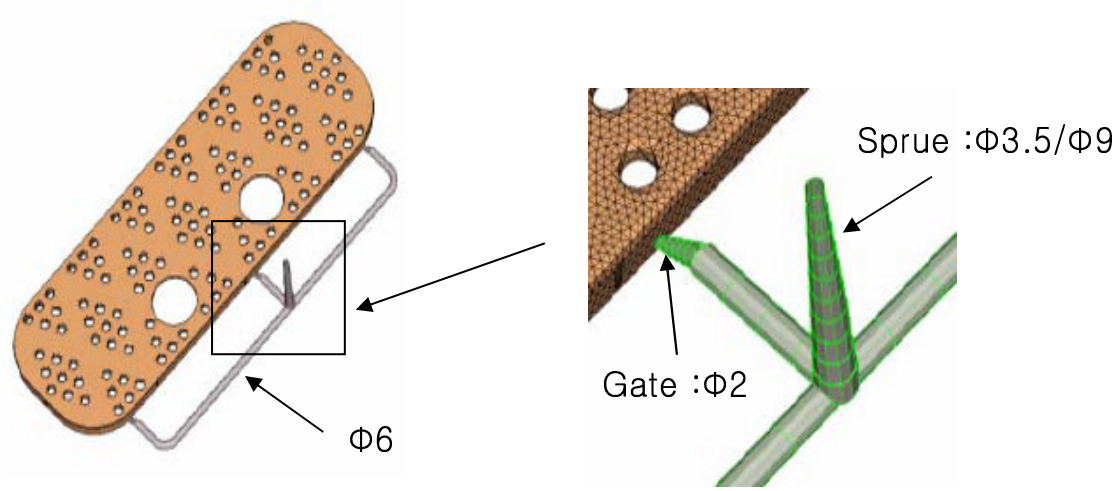

Fig. 17 Analysis model and delivery system

The filling pattern according to the filling time is shown in Fig. 18(a), and the three-point gate system shows imbalanced filling pattern. Two side gates do not contribute considerably to the filling of the molding, and the large weld line is shown in Fig. 18(b). The weld line is usually formed at the contact line at the front part of the flow, and two serious weld lines are formed between the gates. Both the higher injection velocity near the side gates and the injection molding temperature may reduce the weld lines. The deformation at the center of the product is 3mm from the center line, and this is not an acceptable number according to product quality criteria. In the next section, the effects of the different injection velocities, packing pressures, and delivery systems will be discussed.

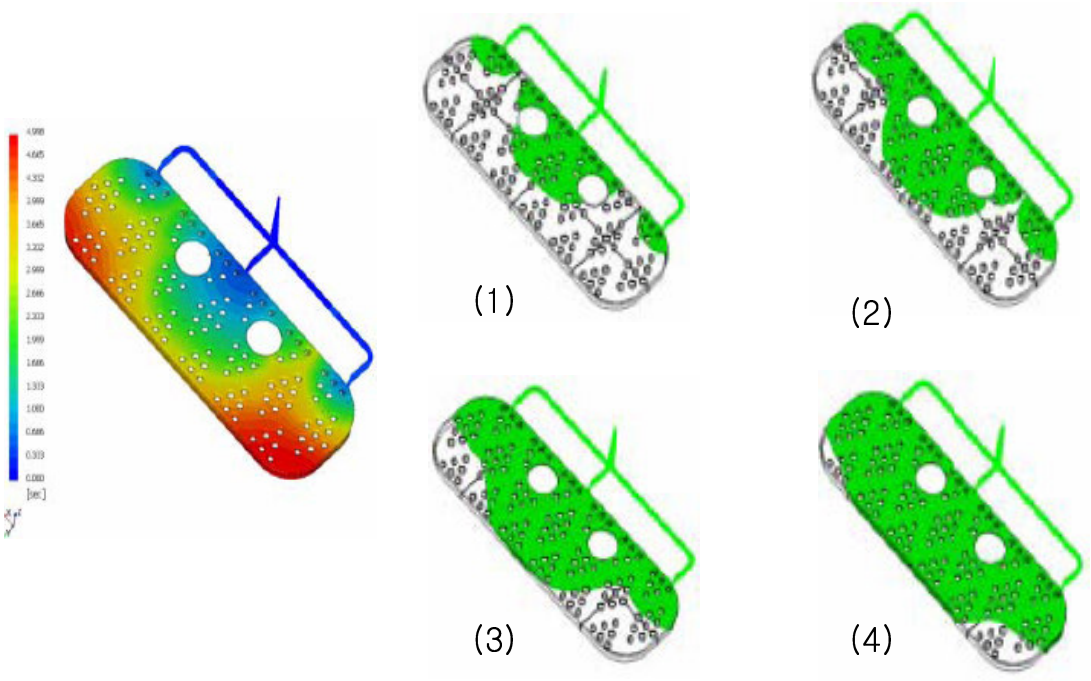

(a) Filling pattern at each time

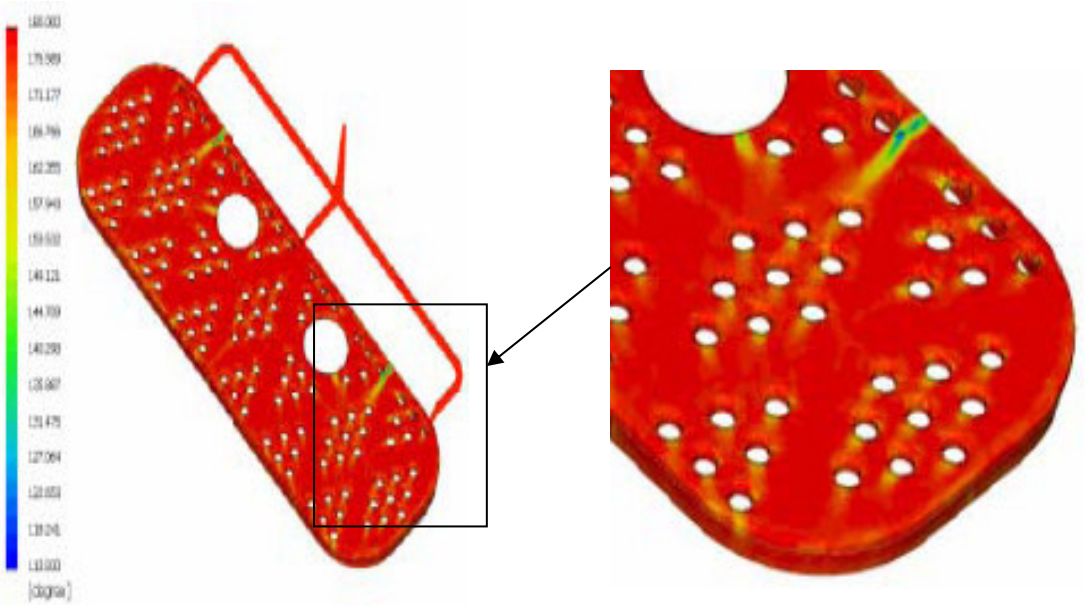

(b) Weld lines between the gates

Fig. 18 Filling pattern and weld lines

- Effect of Injection Molding Conditions

First, three different injection times are used, and Table 5 shows the results of this in flow analysis. Table shows that higher injection time is correlated with lower shear stress; however, the value of the shear stress is not considerable. The injection pressure during the five seconds of injection time is 37.29 MPa, which is an acceptable value for a smaller injection-molding machine. However, in three seconds of injection time, the injection pressure is over 40 MPa. Therefore, the larger injection molding machine should be used to reduce the injection time. The front temperature range during filling for the 5 seconds of injection time is consistent enough to obtain reliably high-quality products. However, the products show 2.857 mm of deformation, which is still high for the product quality criteria.

Table 5 Result for flow analysis for different injection time

	Injection Time = 3 sec	Injection Time = 5 sec	Injection Time = 7 sec
Max. Shear Stress In the part	0.160 MPa	0.151 MPa	0.131 MPa
Max. Shear Rate On the gates	29218 /sec	17531 /sec	12522 /sec
Max. Injection Pressure	42.663 MPa	37.290 MPa	34.337 MPa
Melt Front Temperature Range during Filling	230.98 ~ 228.07 degC	230.76 ~ 226.96 degC	230.63 ~ 224.47 degC

Next, three different packing times are examined, and the shrink ratio reduces as the packing time increases, as shown in Table 6. However, case 2 and case 3 have the same shrink ratio, and the 7 seconds of first packing time are not necessary.

Table 6 Shrinkage ratio for different packing time

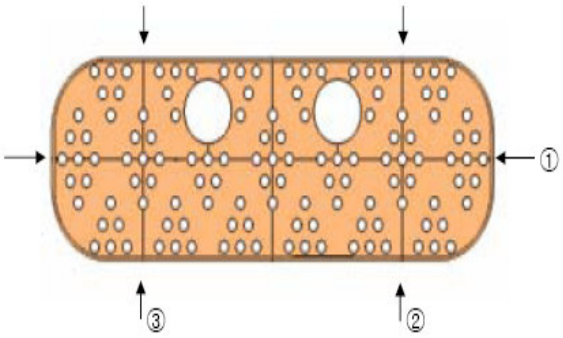

		Distance Before Warp.	Distance After Warp.	Shrink Ratio
3sec	①	380	378.76	0.342
	②	130	129.31	0.529
	③	130	129.33	0.525
5sec	①	380	378.77	0.341
	②	130	129.35	0.521
	③	130	129.35	0.521
7sec	①	380	378.78	0.340
	②	130	129.32	0.515
	③	130	129.30	0.508

Finally, the 2 point gate is used to reduce excessive pressure on the center part, as shown in the 3 point gate. Fig. 19 shows the differences in the filling patterns of the two different gate systems. The 2 point gate has better flow balance than the 3 point gate has. This better flow balance will decrease the size of the weld lines and may reduce the number of weld lines as well. In the next section, the cost-benefit result will be discussed in light of the outcome of current section.

The modeling method using transferred data from CATIA to 3-D TIMON set up by performing this project. The optimization procedure to fabricate a good quality product is established by controlling gate positions, numbers, injection time & filling time for tray grills of water purifiers. The understanding of filling pattern in injection molding analysis is pointed out. Using different injection molding conditions and material selection, $54,000 of manufacturing cost is saved.

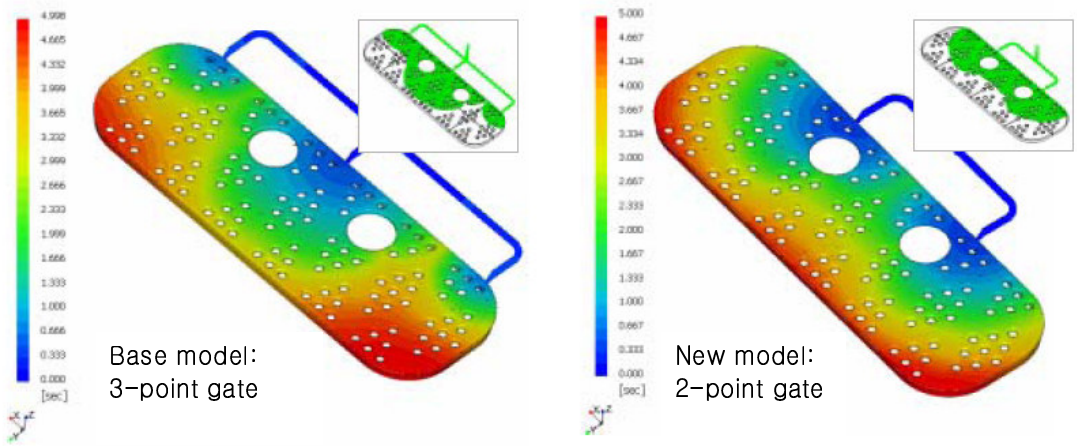

Fig. 19 Difference of the filling pattern for two different gate systems

- Cost-benefit Result

To reduce the cost of production, manufacturing time should be decreased. The shorter injection and packing times are very important factors in reducing the production cost. The use of cheaper materials will aid in this goal as well, and the effects of using cheaper materials may be significant. PC has been used in the production of tray grills to increase their quality. However, the use of ABS in optimized injection molding conditions can create products of equal or better quality. The 30 seconds of cooling time, four seconds of first packing time, and 2-point gate system is used with ABS. In spite of the use of ABS, the deformation of the center part is reduced by about 50%. Its flatness is also improved from 1.8mm to 0.85mm, and the cost savings are shown in Table 7.

Table 7 Cost saving from using ABS

	Price per Kg	Price of total used material	Price per 100,000 products	Cost Saving
PC	$ 2.1	$ 0.54	$ 54,000	$ 54,000
ABS	$ 4.2	$ 1.08	$ 108,000	

CHAPTER V

PROJECT 3: STRESS ANALYSIS OF AN ION−EXCHANGE TANK

5.1 Problem Description

The use of water softener as a home appliance has increased considerably, due to the characteristics of environment-friendly products. In this chapter, numerical and experimental stress analysis will be conducted and studied using FEA and universal test machines. The typical ion-exchange tank is shown in Fig. 20, and the water softener acts on the principle of ion exchange [36-39]. Ions are atoms or groups of atoms that can gain or lose electrons in water and, therefore, exist in water with an electrical charge. Hardness results from calcium (Ca++) and magnesium (Mg++) ions in water.

Ion exchange is a reversible chemical process in which sodium (Na++) ions from the insoluble solid medium (the ion exchanger resin) are exchanged for the calcium and magnesium ions in the water. The physical structure of the resin is not affected. The maximum city water pressure is limited up to 0.49 MPa recommended by city law in KOREA. Therefore, internal pressures up to 0.49 MPa may be applied. The numerical stress analysis is performed using ANSYS in order to study the effects of different configurations of the rib, and the experimental stress analysis is carried out to compare with the results from numerical stress analysis. After the results from numerical and experimental stress analysis have been compared, a numerical stress analysis will be performed in order to estimate the local stress levels for different tank models.

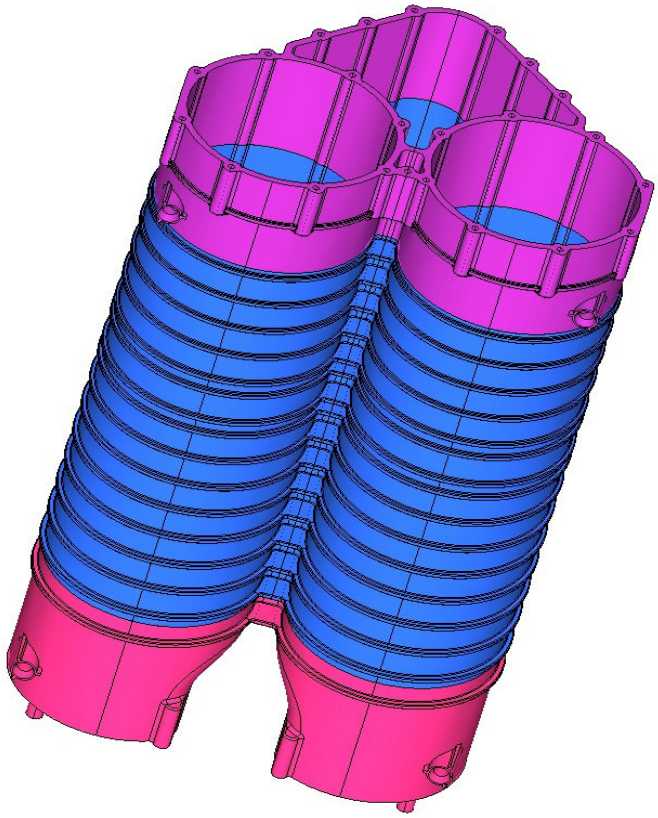

Fig. 20 Typical ion-exchange tank

5.2 Stress Analysis of Ion Exchange Tank with Various Rib Configurations

The commercial finite element analysis software ANSYS is used in the mechanical stress analysis for the ion-exchange tank. The model has 400,000 ten-node tetra elements for the internal pressure loading condition of 0.49 MPa, which is designed to investigate both deformations and stresses. In order to determine the number of elements, a convergence study is performed. The ion exchange tank is basically a pressure vessel. If it is a cylindrical pressure vessel, the hoop stress will have twice the stress level that the longitudinal stress has. The effect of rib according to the position is investigated as shown in Table 8. In this case, only one tank is considered, in order to simplify the problem and save analysis time. The six different models are

studied and the material used is Noryl, which has about 85-120 MPa of material strength. The von Mises stresses and displacements for different models are shown in Table 9. Models 3, 4, and 6 have relatively small displacement as compared to other models. However, models 4 and 6 have very high von Mises stress, which is the same level of material strength. Model 3, which has only hoop-direction ribs, is the best choice

Table 8 Analysis model for ion exchange tank

	Outside of tank		Inside of tank	
	Longitudinal	Hoop	Longitudinal	Hoop
Model 1	X	X	X	X
Model 2	O	X	X	X
Model 3	X	O	X	X
Model 4	O	O	X	X
Model 5	X	X	O	X
Model 6	X	X	X	O

O : rib exists X : no rib

Table 9 Von Mises stress and deformation for different models

	Model 1	Model 2	Model 3	Model 4	Model 5	Model 6
Von-Mises Stress	45 MPa	60 MPa	50 MPa	100 MPa	55 MPa	90 MPa
Displacement	1.125 mm	1.2 mm	0.775 mm	0.897 mm	1.178 mm	0.784 mm

The full model for the ion exchange tank in Fig. 20 is internally pressurized with 0.49 MPa, and the material property is shown in Table 10.

Table 10 Material properties

Material	Young's Modulus	Poisson's Ratio	Tension Strength
Noryl	6000 MPa	0.35	85-120 MPa

Two models are considered, as shown in Fig. 21, and (a) is a base model. Part A in the base model has smaller rib size than part B has. Fig. 21(b) is a modified model that has the same rib size for both part A and part B. The modified model also has extra ribs in part C. The von Misees stress and displacement for the base model is shown in Fig. 22. Point A has the highest value of von Mises stress, and the red-circled area is the weaker part in the ion exchange tank under internal pressure. Therefore, it is possible that the crack begins at point A and grows to the point B in red circle area. The crack initiation and growth will be compared with the experimental data in the next section. The von Mises stress and displacement for modified models are shown in Fig. 23. The strength of the modified model is increased by about 30%, and the displacement is decreased by about 50%, as shown in Fig. 23. Therefore, the modified model has higher strength and lower deformation. The experimental results will be explained and compared with the numerical results in the next section.

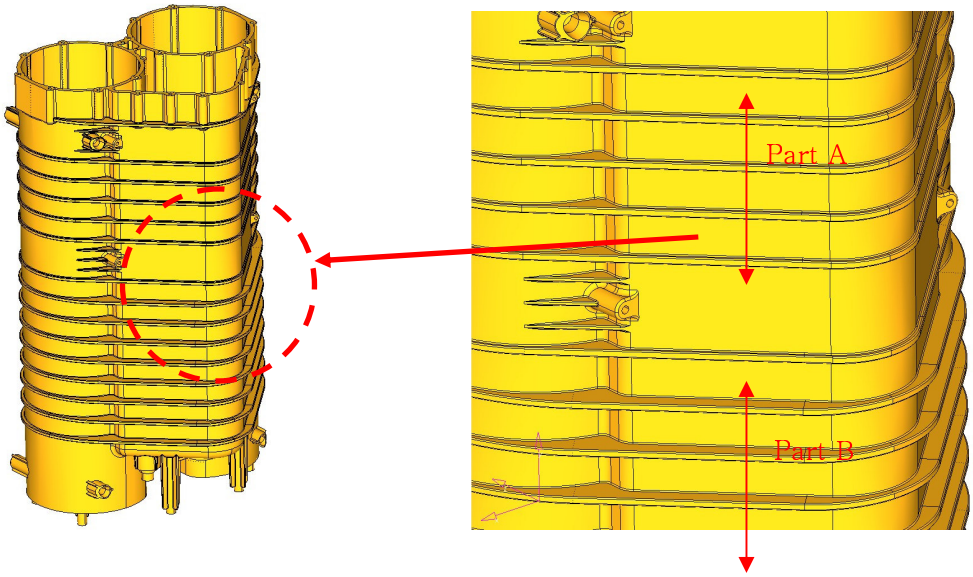

(a) Base Model

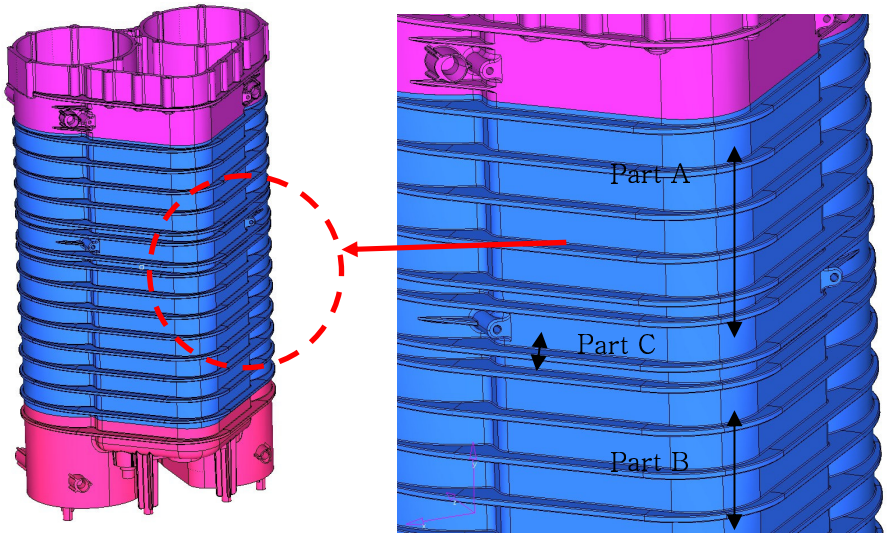

(b) Modified Model

Fig. 21 Base and modified models for ion exchange tank

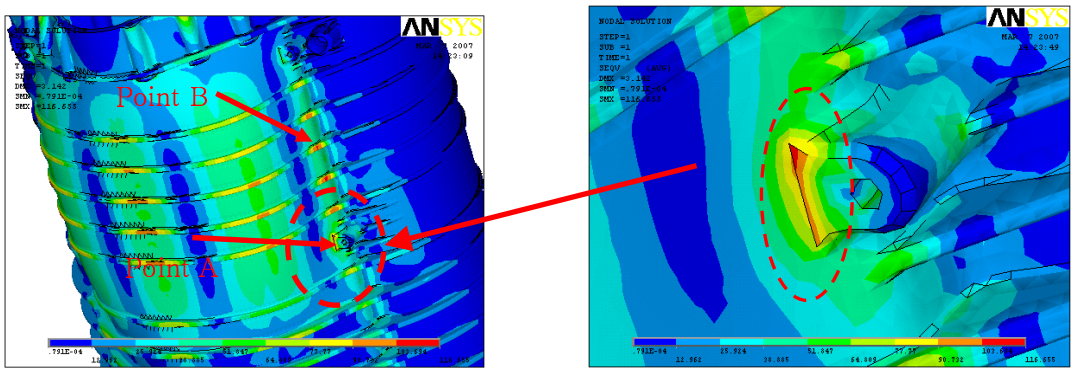

Maximum von Mises Stress: 70 MPa

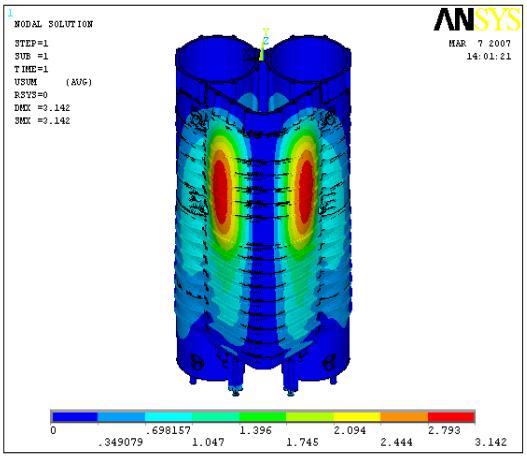

Displacement: 3.142 mm

Fig. 22 Von Mises stress and displacement for base model

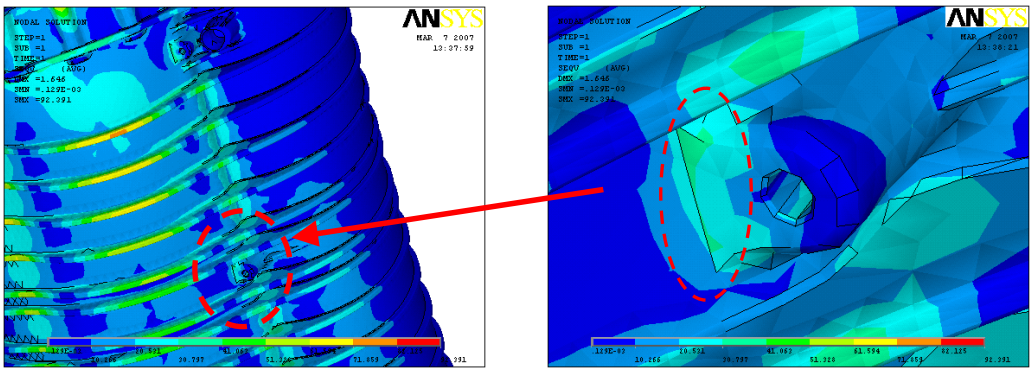

Maximum von Mises Stress: 49 MPa

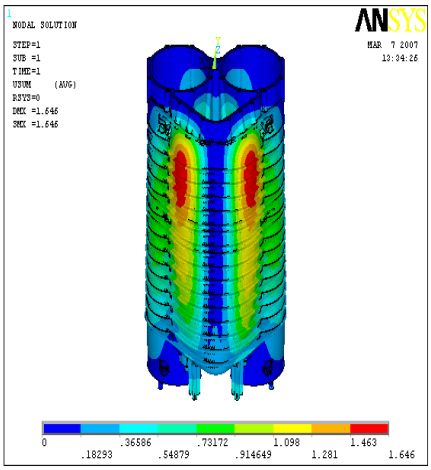

Displacement: 1.646 mm

Fig. 23 Von Mises stress and displacement for modified model

5.3 Experimental Set Up & Results

An in-house universal test machine system has been used to test the ion-exchange tank under internal pressure. The test sample is made by the manufacturing team in Woongjin Coway CO., and the test rig including a pump to pressurize the tank, seating part, and hose is set up by author. The strain gage is attached to the tank in order to compare with the results from the numerical analysis, as shown in Fig. 24. The ion exchange tank is pressurized until there is a fracture, and the fracture strength is 0.69 MPa. The appearance of the fracture in experiments is

very similar to numerical result. The crack begins at point A, and it progresses longitudinally. Even though the experiment is performed until the fracture, only linear numerical analysis is carried out because of the complication and time limit for development schedule. When the experimental result is compared with the numerical value in linear area (Fig. 25), the two are found to be in very good agreement. Therefore, only numerical analysis may be utilized in re-designing an ion exchange tank to increase its strength or performance. It will save the product development time and enhance the ion exchange tank's ability.

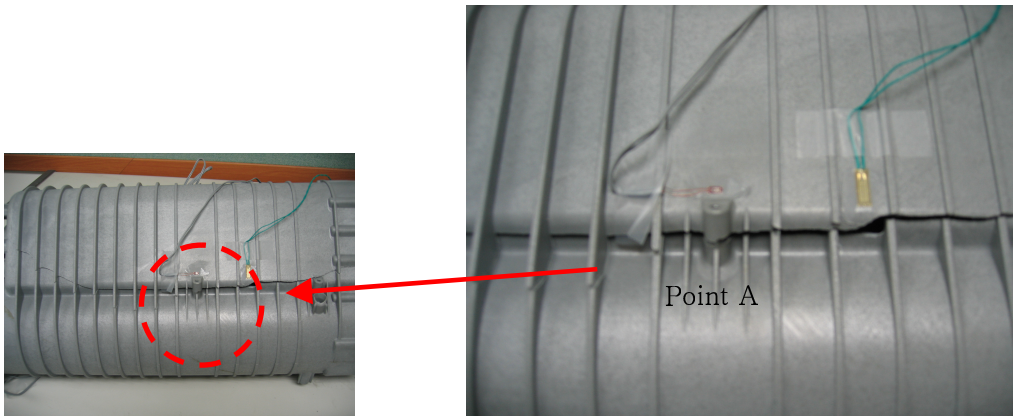

Fig. 24 Ion exchange tank with strain gage

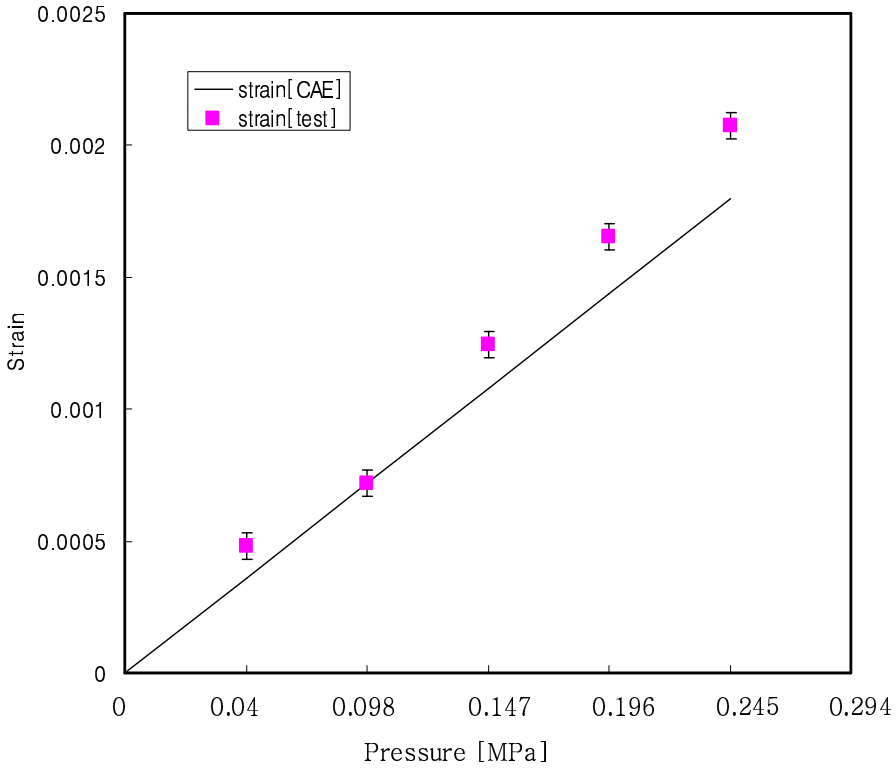

Fig. 25 Comparison between numerical and experimental analysis

CHAPTER VI

PROJECT 4: COST REDUCTION USING SHAPE OPTIMIZATION

6.1 Size and Shape Optimization

The geometric boundary of a structure should be modified in order to solve a shape optimization problem [40, 41]. The morphing technique, which uses OPTISTRUCT, allows us to change meshes through a wide variety of interactive methods, including dragging handles, changing the fillet and hole radii, and mapping an existing mesh to a surface. The OPTISTRUCT, which is a commercial optimization program, has a morphing module that can change shapes and define the shape design variables for OPTISTRUCT shape optimization problems [41-47]. Size and shape optimization involves the movement of nodes, defines within design regions, using user-defined vector perturbations. The movement of the nodes, during optimization, results in a change in the structure. The OPTISTRUCT recognizes every shape that the user has defined, and runs the optimizing steps to find the proper solution. The variables are the range of the thickness or the size, and the responses are, in this case, the stresses and/or the displacement. The responses and variables should be defined before the software is run.

6.2 Problem Description and Optimization Process

The demand for high-quality air purifiers that are suited to new lifestyles has been increasing, and people want to have small, light products. The new air purifiers should demonstrate higher performance and should also be easy to move. Therefore, the general concept for new air purifiers is light and alterative.

Fig. 26 shows the air purifier (product name, NOTOS) and the direction of the air flow. The NOTOS can be used as a stand-up type or lay-down type of purifier, as shown in Fig. 26. In the case of the lay-down type, a child can stand on the front cover and the pressure will be applied

on the air purifier. The purpose of this project is to reduce the product weight in order to decrease the cost, while simultaneously enhancing the product strength to increase toleration of exterior loading.

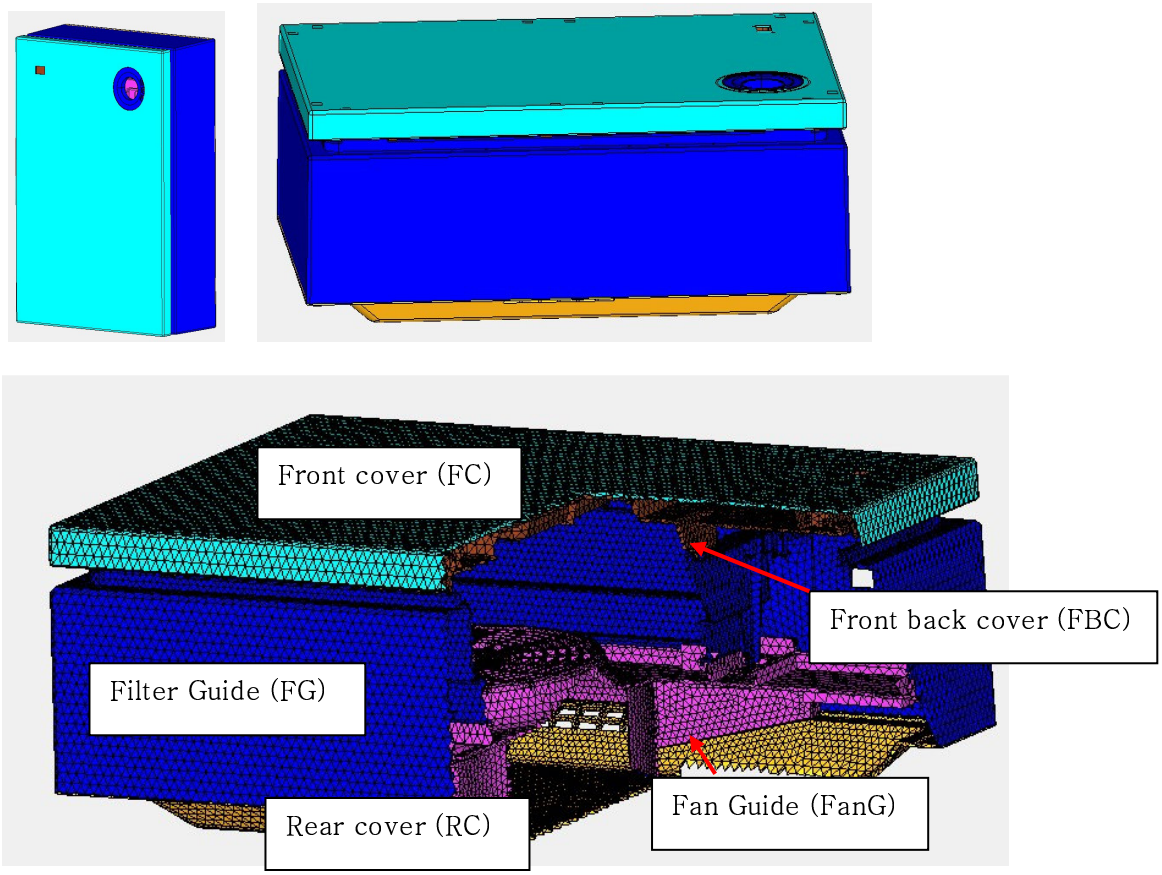

Fig. 26 Configuration of NOTOS model

The optimization process, using OPTISTRUCT, is shown in Fig. 27. After the morphing is finished, the morphing data with loading and boundary conditions should be exported as an ANSYS template data to run a structural analysis. The data will be imported into the OPTISTRUCT for nominal running. The nominal run should be executed in order to create the responses and variables and to evaluate the optimization results.

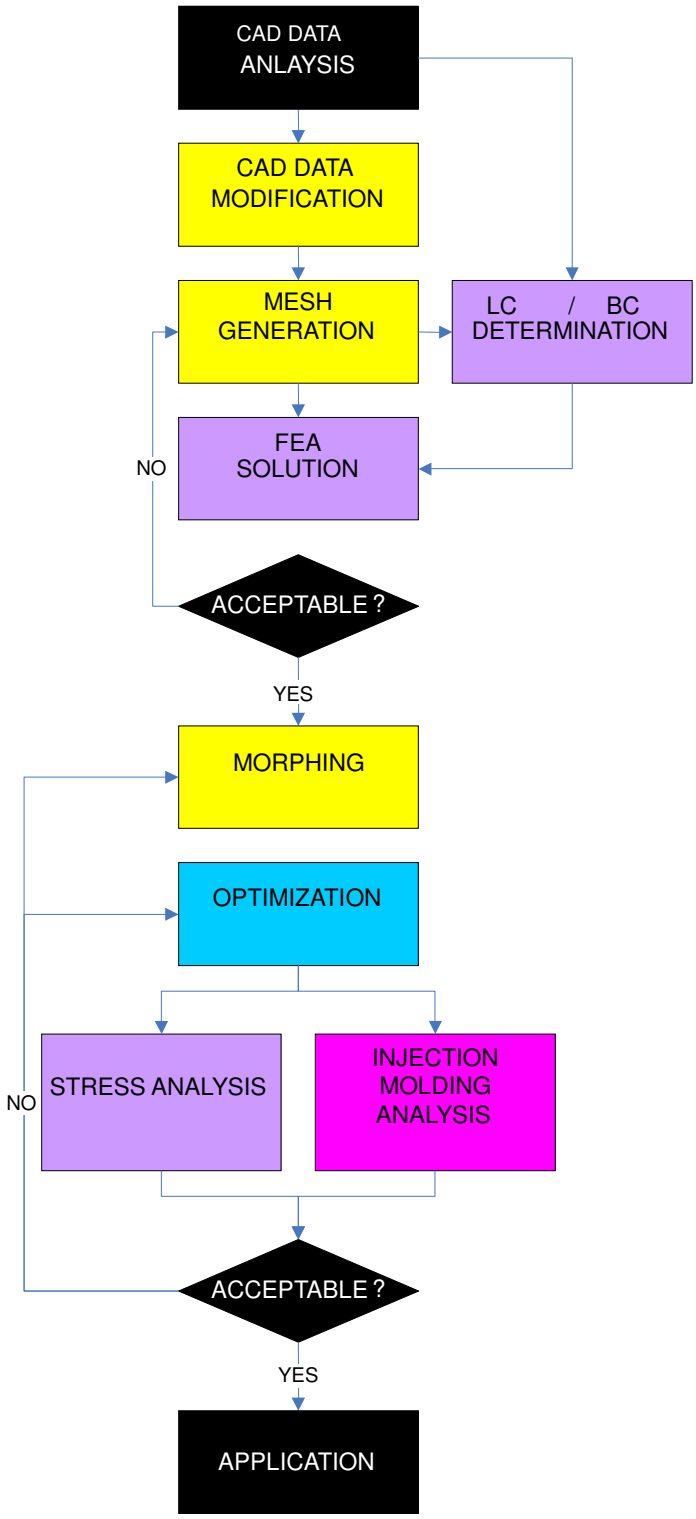

Fig. 27 Optimization process using ANSYS and OPTISTRUCT

6.3 Finite Element Model and Structural Stress Analysis

The commercial finite element analysis software ANSYS is used for the structural stress analysis. The model has 1,000,000 ten-node tetrahedral elements that can be used in all loading conditions to investigate both stresses and deformations. In order to determine the number of elements, a convergence study is performed. The front cover is pressurized, as explained in the previous section, with 0.013 MPa.

The different loading conditions are considered and are shown in Fig. 28. The bottom of the air purifier (part A) is fixed, and the contact boundary conditions are applied as shown in Fig. 29.

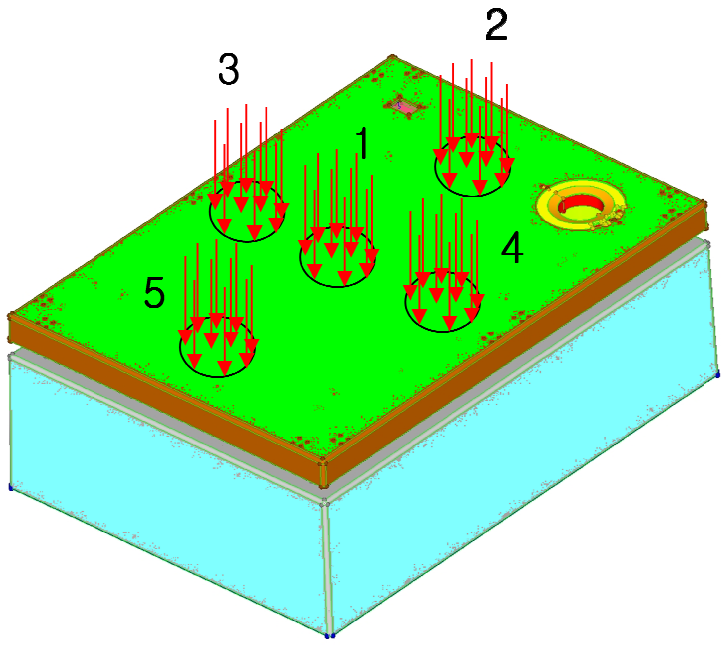

Fig. 28 Five different loading locations

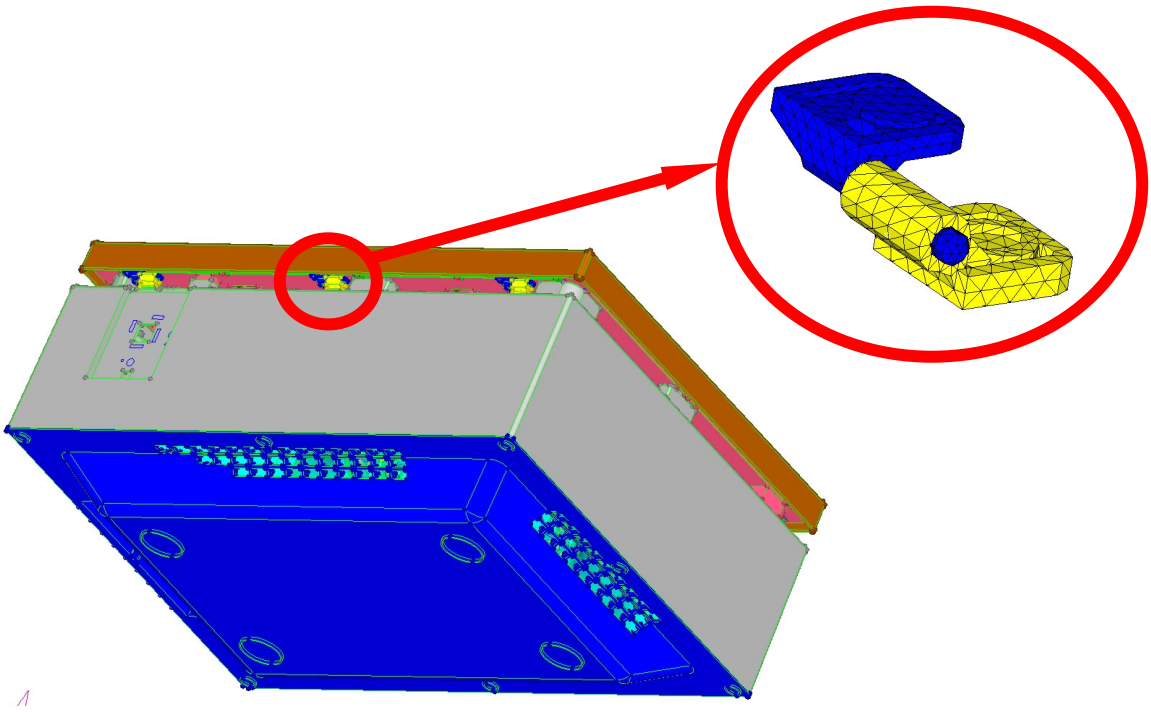

Fig. 29 Contact boundary conditions of hinges

Fig. 30 shows the maximum von Mises stress on the each part under the five different loading conditions. The effective strength for ABS is 20 MPa; therefore, the product is safe for the base model under all loading conditions. The reason that the front cover hinge under left part loading condition has highest value is that the loading is applied to the right upper to the hinge. However, the stress on the hinge is still less than effective strength. The deformation of each part under different loading conditions is also shown in Fig. 31.

In the next section, the stress analysis results after optimization will be introduced, and the final dimension for the each part will be discussed.

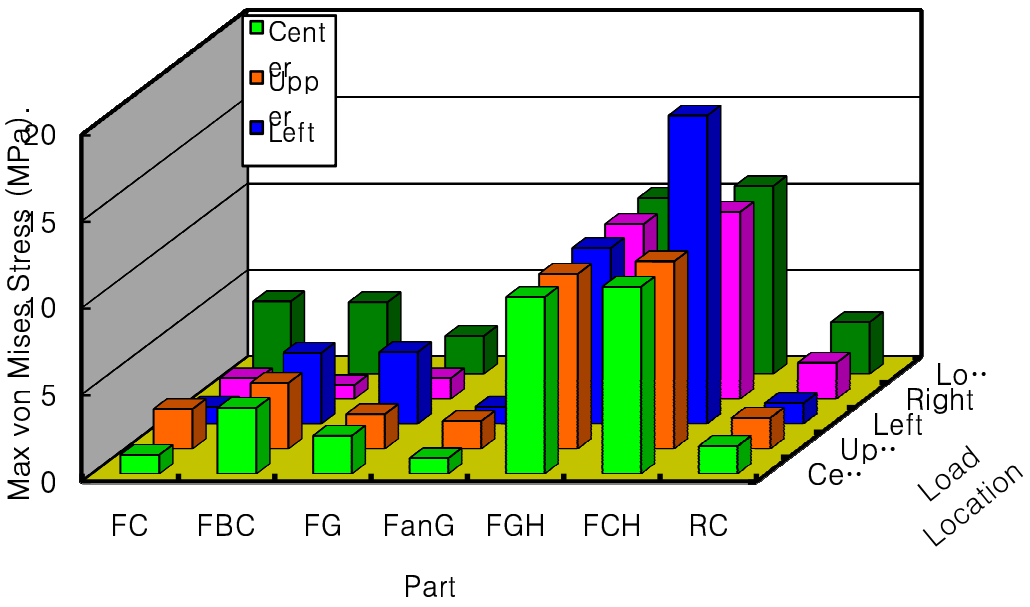

Fig. 30 Von Mises stress of each part for air purifier

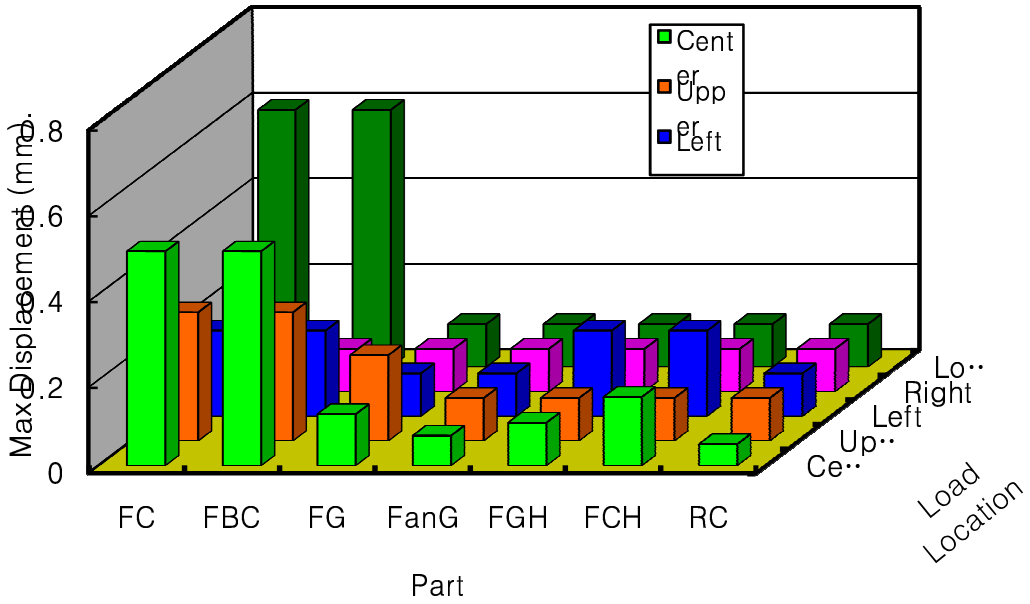

Fig. 31 Deformation of each part for air purifier

6.4 Thickness Optimization

OPTISTRUCT is used to optimize the thickness of the front cover, the front back cover, the filter guide, the fan guide, and the rear cover for NOTOS model. The responses and variables that are used for the optimization are shown in Table 11. The maximum von Mises stress should not exceed the effective strength for ABS, and the deformation should be less than the result from nominal run. The thickness will show variance of up to 20% of the original value.

Table 11 Responses and variables used in optimization

	Front cover, Front back cover, Filter guide, Fan guide, Rear cover
Responses	Maximum von Mises stress, Maximum Displacement
Variables	2.5 – 3.0 mm

The comparison of von Mises stress for before-optimization and after-optimization is shown in Fig. 32. The front back cover and filter guide have a higher stress level after optimization; however, the level is still less than the effective strength. The other parts have an equal or lower value of von Mises stress after optimization even though the parts are thinner in thickness.

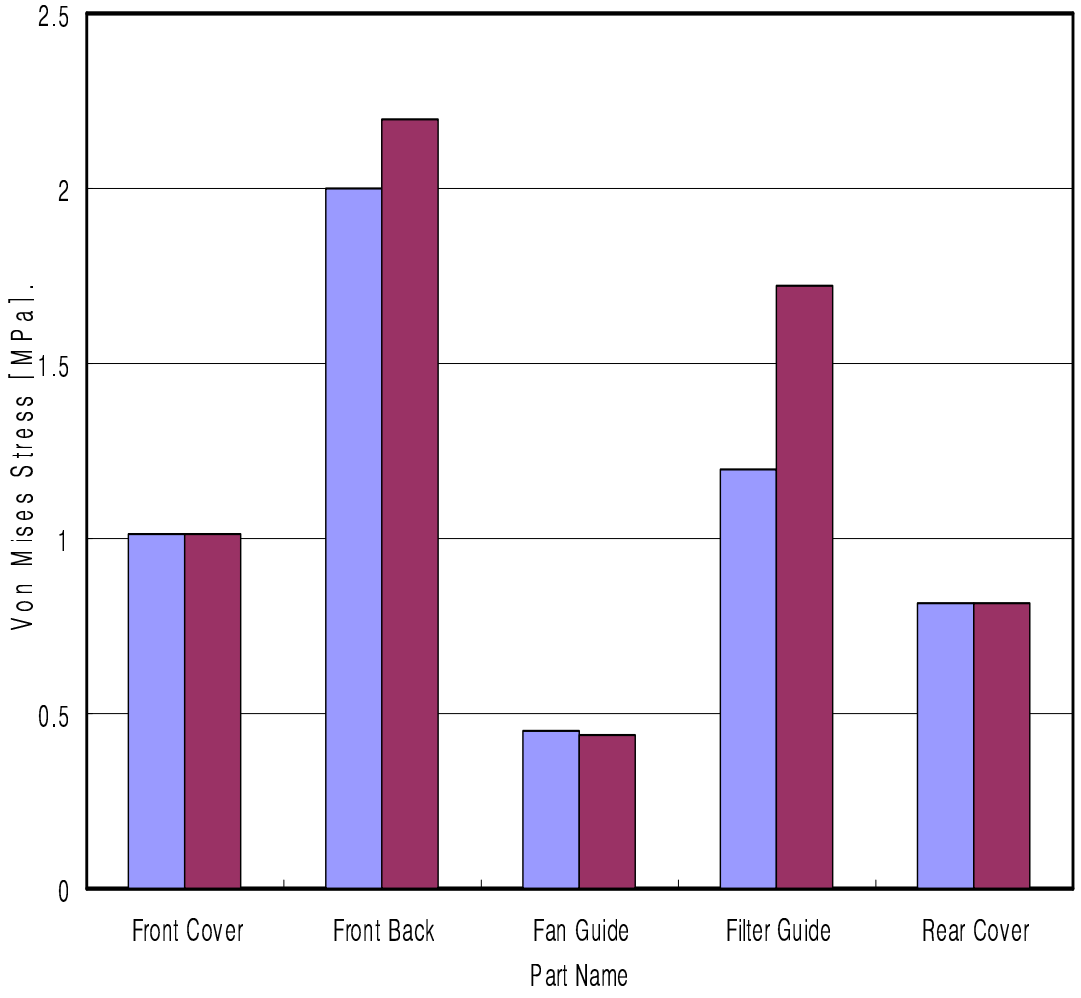

Fig. 32 Comparison of von Mises stress

Fig. 33 shows the comparison of deformations for each part. The response for the deformation is set to less than the result from nominal run; however, the value cannot be lowered in this case. Therefore, the deformation value for both before-optimization and after-optimization has almost same level.

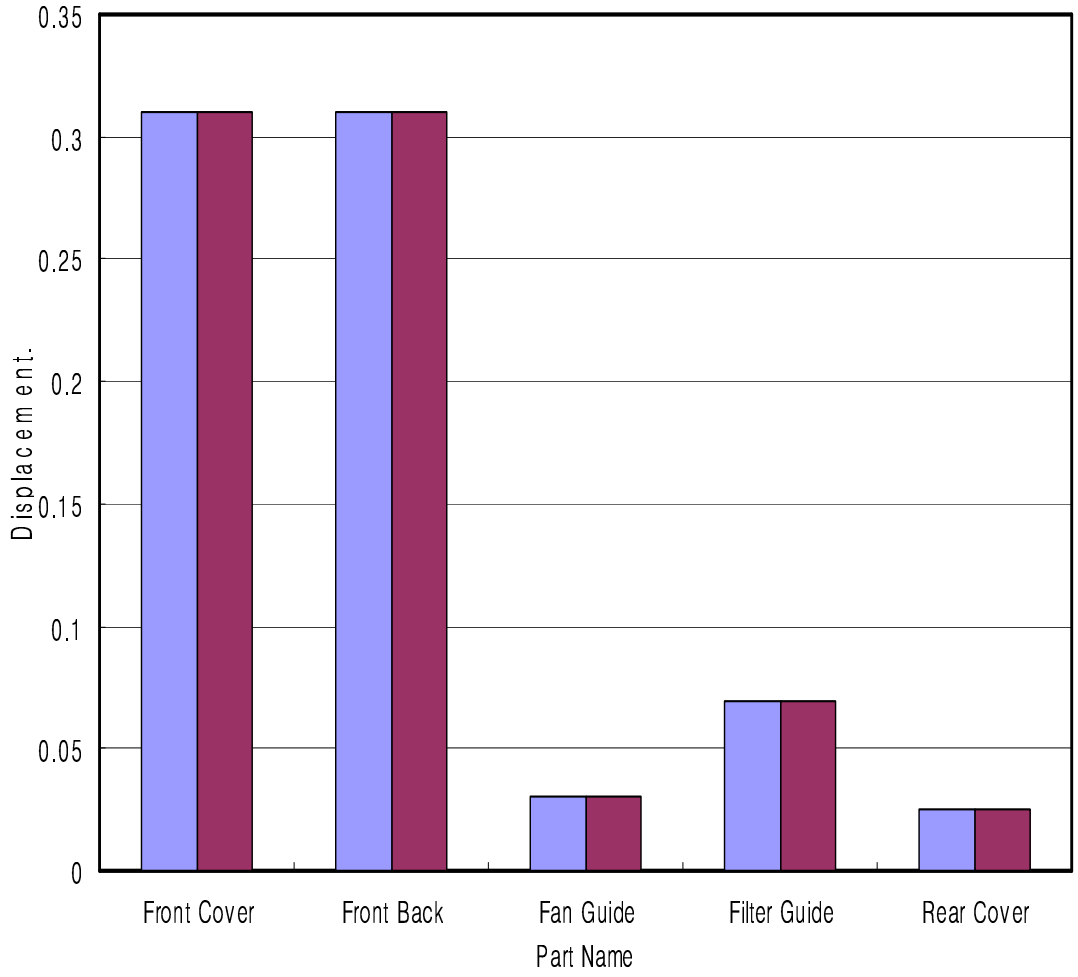

Fig. 33 Maximum deformations for each part in Fig. 26

Fig. 34 shows the thicknesses for each part after optimization, and the fan guide could not be applied for the optimization. The experimental test was performed for the fan guide under actual running conditions, and the noise and vibration level were critical while the fan was operating.

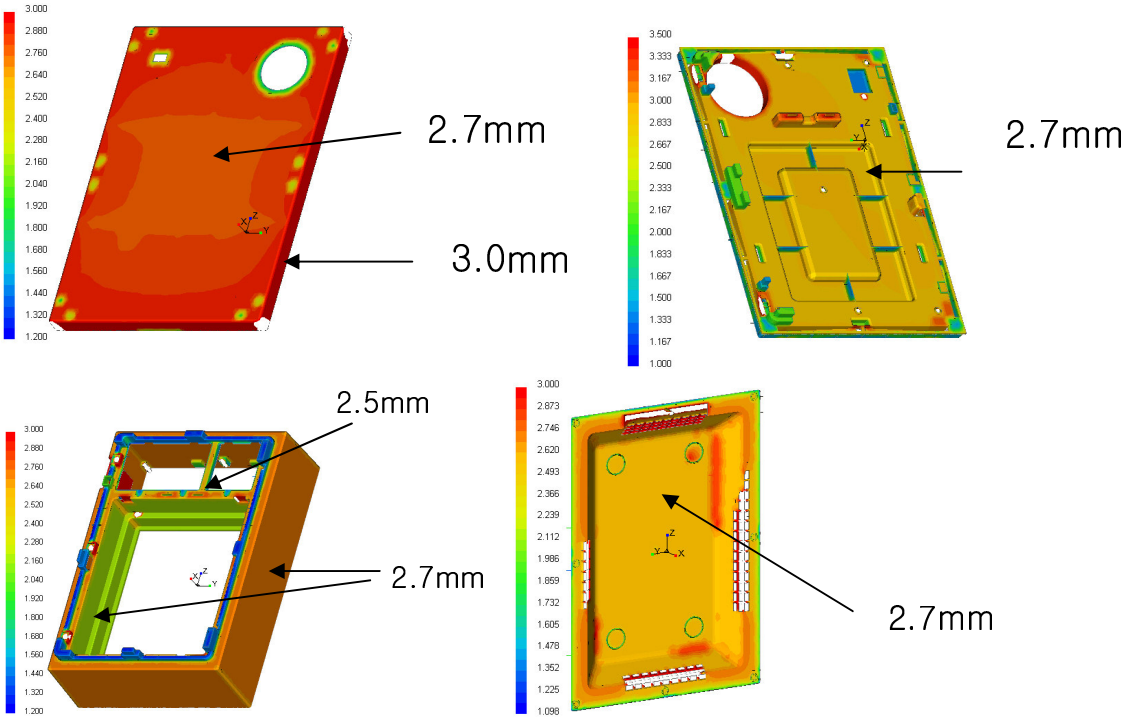

Fig. 34 Thicknesses for each part after optimization

6.5 Injection Molding Analysis

The possibility of mold manufacturing was studied using 3-D TIMON (commercial injection molding software) which is introduced in Chapter Ⅳ, in order to verify the new design of the air purifier. Table 12 and Table 13 show the comparison of each case and of the injection molding conditions and resulting cost savings, respectively. The proper injection molding conditions allow us to make thinner products as well as to obtain better molding results.

Table 12 Injection molding analysis results

	Front Cover		Front Back Cover		Filter Guide		Rear Cover	
	Base	Modified	Base	Modified	Base	Modified	Base	Modified
Filling Time [sec]	5.994	5.935	6.975	6.93	7.985	7.923	4.953	4.951
Clamping Force [ton]	690	650	600	595	360	430	630	510
Deflection [mm]	3.3	4.6	1.506	1.462	3.369	3.679	2.7	3.2

Table 13 Cost saving result

Material	ABS
Amount per Product	8.7 Kg
Cost per Kg	$ 2.57
Cost per Product	$ 22.333
Cost Saving per 100,000 Products	$ 218,300

The optimization method using OPTISTRUCT is developed to reduce the thickness of air purifier system.

-The technique to transfer CATIA file into OPTISTRUCT has been established.

-The solid meshing technique using morphing technology has been set up for topology optimization.

Injection molding analysis is used to verify the results from optimization.

-3-D TIMON is employed to check the possibility of injection molding with different thicknesses of air purifier.

The total weight of air purifier is reduced using optimization method.

-8.7 kg per product is reduced, and it saves about $218,300 a year.

-The maximum von Mises stress in air purifier under general usage condition (described in section 6.2) is same or decreased after optimization.

CHAPTER VII

NEW DEVELOPMENT PROCESS USING CAE

7.1 Typical Development Process

The purpose of this project is to reduce the development time as optimize the development process. My job is to develop new process using CAE technology.

First, I gathered and analyzed all development related information, and analyzed down the problems that the current process has. After that, the research & development department is reorganized after interviewing team leaders, high-level managers, and CEO. The current development process is explained as follows.

The typical total development time for mass production is usually about eight months, as shown in Fig. 35. The 2-D design team first calls a meeting for the purpose of exploring product planning intention, realization-possibility, and production-possibility. The product planning team and product development team are included in this meeting, and the marketing department will assist in the decision as well. After the design team finalizes the model, the product development team will verify the system/part design for product development concept and goal. The product development team creates the 3-D design using CATIA (commercial computer aided design software). The specification for the product system and parts will be finalized before the first design review is called. The test sample will be designed to measure reliability, safety, and productivity. After confirming the quality of the mold and checking the reliability of the new parts, the final production will be placed. However, the product development time usually takes more than eight months, as the mold may not be perfect, the product may have a defect, or the product may have lower strength than it should have.

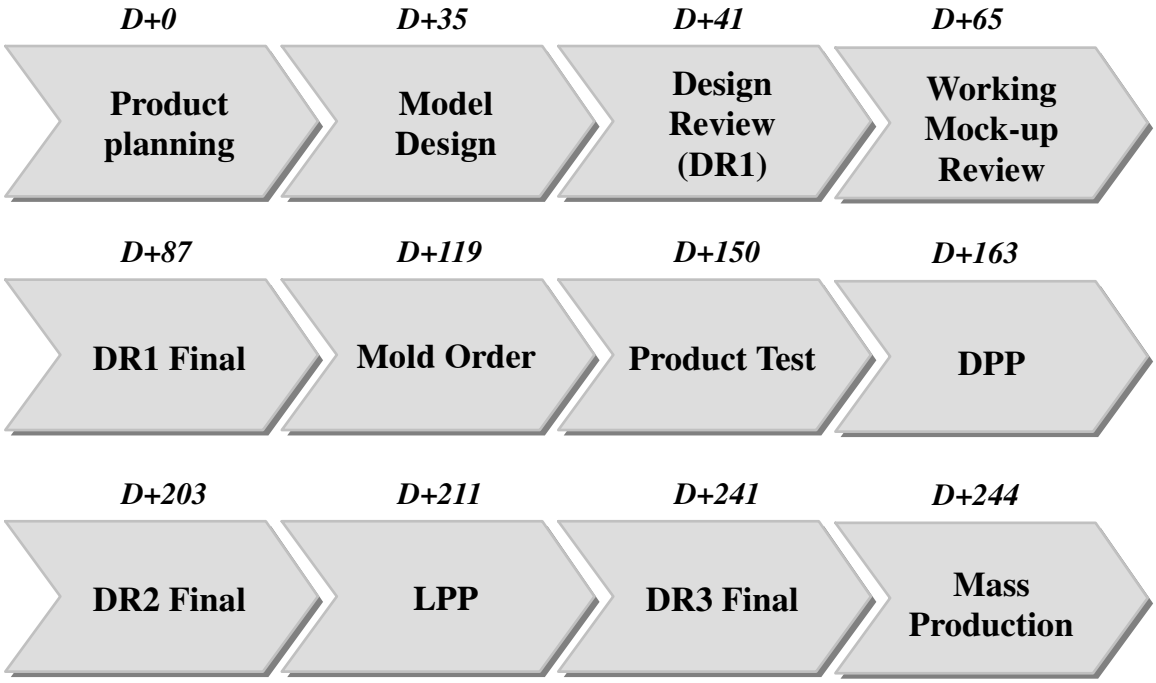

Fig. 35 Development flow chart

7.2 Proposal of New Development Process [48-51]

The cost for a working mock-up is usually about $100,000, and when there is a defect in the design, this cost will be doubled. The development time will be increased as well. This is the reason that the first CAE result should be reported and reflected before a working mock-up is ordered as shown in Fig. 36. The second CAE process should be finished when the final design review has been placed. This will lead to better design and improved product quality, as well as decreases in the development time and cost. The most important element is the education of designers on product development team, to ensure that they are involved in this process both directly and indirectly. The whole product design team will be changed and the production time may be longer than before, because the scope of their jobs has increased. However, this new process will make their jobs easier and better. This project is still ongoing and it will save significant amount of money and time if it is successful.

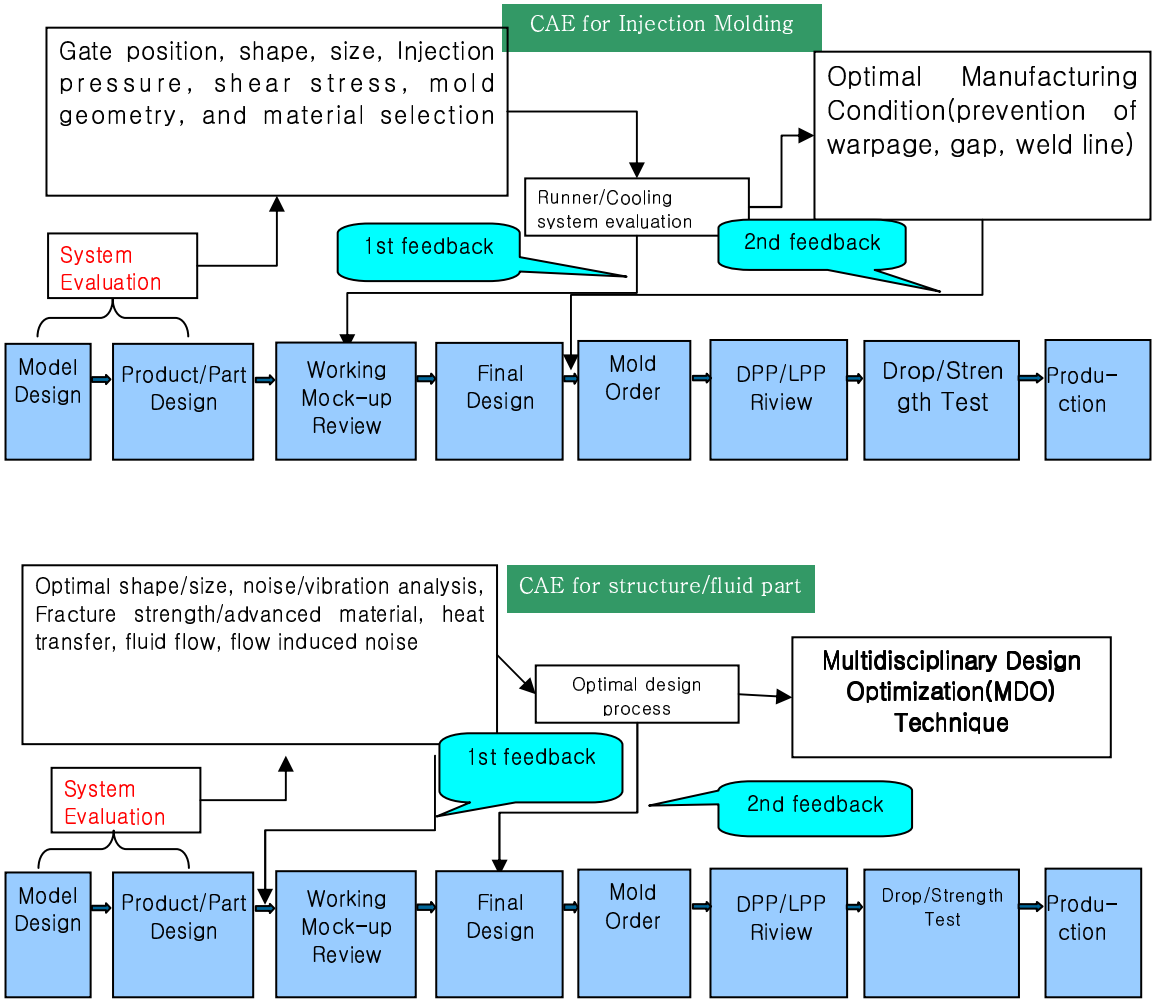

Fig. 36 Proposed development process with CAE environment

CHAPTER VIII

SUMMARY AND CONCLUSIONS

The following conclusions could be drawn through this report:

The MDO (Multi Disciplinary Optimization) technique to reduce production cost and developing time was introduced.

PROJECT 1:

1. A new insert model for the fan of air purifier systems was developed and the reliability test results showed a good agreement with numerical stress analysis.
2. CATIA is used for designing air purifier system, and ALGOR is utilized to analyze thermomechanical problem.
3. ALGOR showed high compatibility with CATIA for transferring 3-D CAD model.

PROJECT 2:

1. The 50% of production cost was trimmed down for the tray grill of water purifier systems using optimized injection molding conditions
2. CATIA is used for designing tray grill of water filtrating system, Hypermesh is used to build a tetra mesh, and 3-D TIMON solver is utilized for injection molding analysis.

PROJECT 3:

1. The numerical stress analysis was correlated with experimental results for the ion-exchange tank, and both results are in very good agreement.
2. ANSYS is employed because it has high ability of parametric mesh morphing.
3. The possibility for using hoop directional ribs is verified to increase the strength of ion-exchange tank.

PROJECT 4:

1. The shape optimization method and procedure using OPTISTRUCT and ANSYS was

proposed, and the overall product thickness was reduced by up to 20% of the original thickness.

2. Hypermesh is applied to build a 3-D solid mesh and morphing control points, ANSYS and OPTISTRUCT are utilized for shape optimization of air purifier system. ANSYS is used for structural analysis and parametric mesh morphing. OPTISTRUCT is used for automation of shape optimization, and reducing analysis time.
3. $218.300 of material cost is saved using shape optimization, and the overall strength is not affected. The maximum von Mises stress is even decreased for several parts of air purifier.

Additional work is needed in order to increase the accuracy of numerical and experimental stress analysis. The optimization procedure will be modified to make the process fast and precise.

1. Measurement of material properties, including Young's modulus, tensile strength, and the fatigue limit for plastics.
2. Experimental apparatus for filter, ion-exchange tank, and nozzle etc.
3. Automation of optimization procedure
4. Validation of new development process by performance and comparison with the previous development process.

REFERENCES

[1] Balling, R. J., and Sobieszczanski-Sobieski, J., "Optimization of coupled systems: a critical overview of approaches," *AIAA Journal*, Vol. 34, No. 1, 1996, pp. 6-17.

[2] Sobieszczanski-Sobieski, J., and Haftka, R. T., "Multidisciplinary aerospace design optimization: Survey of recent developments," *Structural Optimization*, Vol. 14, 1997, pp. 1-23.

[3] Geiger, T. S., and Dilts, D. M., "Automated design-to-cost: Integrating costing into the design –decision," *CAD Comput Aided Design,* Vol. 28, No. 6-7, 1996, pp. 423-438.

[4] Kassapoglou, C., "Simultaneous cost and weight minimization of composite- stiffened panels under compression and shear," *Compos Part A: Appl Sci Manuf*, Vol. 28, No. 5, 1997, pp. 419-435.

[5] Kassapoglou, C., "Minimum cost and weight design of fuselage fames. Part A: design constraints and manufacturing process characteristics," *Compos Part A: Appl Sci Manuf,* Vol. 30, No. 7, 1999, pp. 887-894.

[6] Gantois, K., and Morris, A. J., "The multi-disciplinary design of a large-scale civil aircraft wing taking account of manufacturing costs," *Struct Multidisciplinary Optim,* Vol. 28, 2004, pp. 31-46.

[7] Park, C. H., Lee, W. I., Han, W. S. and Vautrin, A., "Simultaneous optimization of composite structures considering mechanical performance and manufacturing cost," *Compos Struct*, Vol. 65, No. 1, 2004, pp. 117-127.

[8] Kou, X. Y. and Tan, S. T., "A systematic approach for integrated computer-aided design and finite element analysis of functionally-graded-material objects," *Materials and Design,* Vol. 28, 2007, pp. 2549-2565.

[9] Sai, Z., "Knowledge-based FEA modeling for highly coupled variable topology multi-body

problems," Ph.D. dissertation, Georgia Institute of Technology, 2004.

[10] Rong-Sheng, C., Chen-Yi, T., and Guey-Shin, C., "The residual thermal stresses due to - cool-down of post cure for the symmetric cross-ply TCM composite material," *Composite Structures,* Vol. 26, 1993, pp. 155-166.

[11] Yu-Cheng, L., Hesketh[a] , P. J., and Schuster[b], J. P., "Finite-element analysis of thermal stresses in a silicon pressure sensor for various die-mount materials," *Sensors and Actuators A,* Vol. 44, 1994, pp. 145-149.

[12] Szyszkowski, W., and King, J., "Stress concentrations due to thermal loads in composite materials," *Computers & Structures,* Vol. 56, No. 2/3, 1995, pp. 345-355.

[13] Yang, Y.Y., and MUNZ, "Stress singularities in a dissimilar materials joint with edge tractions under mechanical and thermal loaings," *Int. J. Solids Structures,* Vol. 34, No. 10, 1997, pp. 1199-1216.

[14] Bogy, D. B., "Two edge-bonded elastic wedges of different materials and wedge angles under surface traction," *Translations ASME, Journal of Applied Mechanics,* Vol. 38, 1971, pp. 377-386.

[15] Yang, S. S., and Kwon, T. H., "A study of birefringence, residual stress and final shrinkage for precision injection molded parts," *Korea-Australia Rheology Journal*, Vol.19, No.4, 2007, pp. 191-199.

[16] Santa Clara University, School of Engineering: The Engineering Design Center, *Residual stresses section, 2003,* http://www.scudc.scu.edu/cmdoc/dg_doc/develop/process/physics/b3400001.htm, July 5th, 2008.

[17] Frank, P. Baaijens, and Lucien, F. A. Douven, "Calculation of flow-induced residual stresses in injection moulded products," *Springer Netherlands*, Vol. 48, 1994, No. 2.

[18] Higdon, A., Ohlsen, E. H., Stiles, W. B., Weese, J. A. and Riley, W. F., *Mechanics of*

Materials, 3rd ed., John Wiley & Sons, New York, 1976.

[19] Kalev, I., "Cyclic plasticity and fatigue of structural components," *AIAA Journal*, Vol. 18, No. 10, 1981, pp. 869-873.

[20] Seqalman, D., and Reese, G.., "Estimating the probability distribution of von Mises stress for structures undergoing random excitation. Part I: Derivation," *International Mechanical Engineering Congress and Exposition*, 1998, pp. 15-20.

[21] Rotenberg, R. R. P., "Development process of seamless airbag covers," Internship Report, Eindhoven University of Technology, Report MT 04.13 , July 2004.

[22] Ward, I. M., "Mechanical Properties of Solid Polymers," *Wiley InterScience*, London, 1971.

[23] Tsarina, C. C., and Nimmer, R., *Structural Analysis of Thermoplastic Components,* McGraw-Hill Inc., 1994.

[24] Bicerano, J., *Prediction of Polymer Properties*, Marcel Dekker Inc., New York, 2002.

[25] Mascia, L., and Xanthos, M., **"**An overview of additives and modifiers for polymer blends: Facts, deductions, and uncertainties," *Adu. Polym. Technol,* Vol. 11, No. 4, 1992, pp. 237.

[26] Crawford, R. J., *Plastics engineering,* 2nd ed., Pergamon Press, Oxford, 1987.

[27] Carty, P., and White, S., "The effect of DOP plasticizer on smoke formation in poly(vinyl chloride)," *Polymer,* Vol. 33, No. 5, 1992, p. 1110.

[28] Paul, D. R., Barlow, J. W., and Kekkula, H., *Encyclopedia of Polymer Science and Engineering,* Vol. 12, Wiley, New York, 1988.

[29] Hornsby, P. R., "Thermoplastics structural foams," *Materials & Design*, Vol. 3, Issue 1, 1982, pp. 354-362.

[30] Hetu, J., and Ilinca, F., "Three dimensional modeling and simulation of injection molding process," *15th AIAA Computational Fluid Dynamics Conference*, Anaheim, California, June 2001.

[31] Herber, C. A., and Shen, S. F., "A finite element/finite difference simulation of the injection molding filling process," *J. Non-Newtonian Fluid Mechanics*, Vol. 7, 1980, pp. 1-32.

[32] Dupret, F., Couiot, A., Mal, O., Vanderschuren, L., and Verhoyen, O., "Modeling and simulation of injection molding," In D. De Kee, D.A. Siginer, and R.P. Chhabra, editors, *Advances in the Flow and Rheology of Non-newtonian Fluids*, Rjeology Series. Elsevier, Amsterdam, 1998.

[33] Hetu, J. F., Gao, D. M., Garcia-rejon, A., and Salloum, G., "3D finite element method for the simulation of the filling stage in injection molding," *Polymer Engineering and Science*, Vol. 38, No. 2, 1998, pp. 223.

[34] Chang, R. Y. and Yang, W. H., "Numerical simulation of mold filling in injection molding using a three-dimensional finite volume approach," *International Journal for Numerical Methods in Fluids*, Vol. 37, 2001, pp. 125.

[35] Haagh, G. A. A. V., Peters, G. W. M., Van De Vosse, F. N., and Meijer, H. E. H., "A 3-D finite element model for gas-assisted injection molding: Simulations and experiments," *Polymer Engineering and Science*, Vol. 41, No. 3, 2001, pp. 449.

[36] Prajapati, M. N., Gaurand, P.M. and Dasare, B. D., "Brackish water desalination by a continuous counter-current ion-exchange technique," *Desalination*, Vol. 52, 1985, pp. 317-326.

[37] Francis, X. M., and Fisher, S. A., "Measurements and control in ion exchange installations," *Desalination*, 1986, pp. 403-424.

[38] Applebaum, S. B., "Demineralization by ion exchange," *Academic Press*, 1968, pp. 47-53.

[39] Nachod, F. C., "Ion exchange technology," Academic Press Inc., 1956, p. 245.

[40] Schramm, U., Poh-Soong, Z. T., and Cathal G. H., "Topology layout of structural design and buckling," *10th AIAA/ISSMO Multidisciplinary Analysis and Optimization Conference,*

AIAA 2004-4636, Sep. 2004.

[41] Sigmund, O. and Peterson, J., "Numerical instabilities in topology optimization: A survey on procedures dealing with checkerboards, mesh-dependencies and local minima," *Struct. Optim.,* Vol. 16, 1998, pp. 68-75.

[42] Torstenfelt, B., and Klarbring, A., "Conceptual optimal design of modular car product families using simultaneous, shape and topology optimization," *Finite Elements in Analysis and Design,* Vol. 43, 2007, pp. 1050-1061.

[43] Krog, L., Tucker, A., and Rollema, G., "Application of topology, sizing and shape optimization methods to optimal design of aircraft components," *Proc. 3rd Altair Engineering UK HyperWorks User's Conference*, Bristol, UK, 2002.

[44] Bendsoe, M. P., and Mota Soares, C. A., *Topology Design of Structures*, NATO ASI Series, Kluver Academic Publishers, Dortdrecht, The Netherlands, 1993.

[45] Bendsoe, M. P., *Optimisation of structural topology, shape and material*, Springer-Verlag, Heidelberg, Germany, 1995.

[46] Zhen, L., Jingzhou, Y., and Liping, C., "A new procedure for aerodynamic missile designs using topological optimization approach of continuum structures," *Aerospace Science and Technology,* Vol. 10, 2006, pp. 364-373.

[47] Kilian, S., Zander, U., and Talke, F. E., "Suspension modeling and optimization using finite element analysis," *Tribology International,* Vol. 36, 2003, pp. 317-324.

[48] Purushothaman, N., Menon, M., Pandle, P., Rivard, C., and Chen, H., "High confidence performance prediction to improve the vehicle development process," VC3 CAE, Ford Motor Company, *MSC 1996 World User's Conference Proceedings*, Newport Beach, California, US, 1996.

[49] Ojala, J. K., "Using ABAQUS in tire development process," Nokian Tyres plc., R&D/Tire

Construction, *2005 ABAQUS Users' Conference,* Hilton Slussen, Stockholm, Sweden, 2005.

[50] Moser A., and Schwelger R., "Prospects and Barriers for Up-front CAE-simulation in the Automotive Development," AutoSIM Project funded by European Commission, http://www. Vif tugraz.at/ content/ news/ files, Oct. 24th, 2008.

[51] Schelkle, E., and Elsenhans, H., "Virtual vehicle development in the concept stage current status of CAE and outlook on the future," *3RD MSC Worldwide Aerospace Conference & Technology Showcase*, September 24-26, 2001 Toulouse, France.

VITA

Name: BONG TAEK OH

Address: Texas A&M University
Department of Aerospace Engineering
H.R. Bright Building, Rm. 701, Ross Street - TAMU 3141
College Station TX 77843-3141

Email Address: btoh@koreaaero.com

Education: B.S., Mechanical Engineering, Soongsil University, 1994
M.S., Mechanical Engineering, Soongsil University, 1996
D.En., Engineering, Texas A&M University, 2009